11-2019

Role of The Cortex in Visuomotor Control of Arm Stability

Dylan B. Snyder
Marquette University

Scott A. Beardsley
Marquette University, scott.beardsley@marquette.edu

Brian D. Schmit
Marquette University, brian.schmit@marquette.edu

Role of The Cortex in Visuomotor Control of Arm Stability

Dylan B. Snyder
Department of Biomedical Engineering, Marquette University and Medical College of Wisconsin, Milwaukee, Wisconsin

Scott A. Beardsley
Department of Biomedical Engineering, Marquette University and Medical College of Wisconsin, Milwaukee, Wisconsin

Brian D. Schmit

Department of Biomedical Engineering, Marquette University and Medical College of Wisconsin, Milwaukee, Wisconsin

Abstract

Whereas numerous motor control theories describe the control of arm trajectory during reach, the control of stabilization in a constant arm position (i.e., visuomotor control of arm posture) is less clear. Three potential mechanisms have been proposed for visuomotor control of arm posture: *1*) increased impedance of the arm through co-contraction of antagonistic muscles, *2*) corrective muscle activity via spinal/supraspinal reflex circuits, and/or *3*) intermittent voluntary corrections to errors in position. We examined the cortical mechanisms of visuomotor control of arm posture and tested the hypothesis that cortical error networks contribute to arm stabilization. We collected electroencephalography (EEG) data from 10 young healthy participants across four experimental planar movement tasks. We examined brain activity associated with intermittent voluntary corrections of position error and antagonist co-contraction during stabilization. EEG beta-band (13–26 Hz) power fluctuations were used as indicators of brain activity, and coherence between EEG electrodes was used as a measure of functional connectivity between brain regions. Cortical activity in the sensory, motor, and visual areas during arm stabilization was similar to activity during volitional arm movements and was larger than activity during co-contraction of the arm. However, cortical connectivity between the sensorimotor and visual regions was higher during arm stabilization compared with volitional arm movements and co-contraction of the arm. The difference in cortical activity and connectivity between tasks might be attributed to an underlying visuomotor error network used to update motor commands for visuomotor control of arm posture.

NEW & NOTEWORTHY We examined cortical activity and connectivity during control of stabilization in a constant arm position (i.e., visuomotor control of arm posture). Our findings provide evidence for cortical involvement during control of stabilization in a constant arm position. A visuomotor error network appears to be active and may update motor commands for visuomotor control of arm posture.

INTRODUCTION

Visuomotor control of arm posture might involve cortical structures that provide motor commands to correct errors in position. During movement, agonist muscles are activated to move the limb toward the target, which is followed by antagonist muscle activation to provide braking. Whereas numerous motor control theories describe the control of arm trajectory during a reach (Feldman 1986; Flash and Hogan 1985; Houk et al. 2000; Kalaska et al. 1997; Latash et al. 2010; Todorov and Jordan 2002), the control of the stabilization phase after the end of the movement is less clear. At least three possible mechanisms have been proposed for visuomotor control of arm posture: *1*) increased impedance of the arm through

the co-contraction of antagonistic muscles (e.g., Franklin et al. 2004), *2*) spinal or supraspinal reflex circuits to provide corrective muscle activity (Kurtzer et al. 2008), and/or *3*) intermittent voluntary corrections to errors in position (Hasan 2005). In this study, we examined electroencephalography (EEG) data during a series of arm stabilization tasks to test the hypothesis that cortical error correction networks are involved in visuomotor control of arm posture.

Each of the proposed mechanisms of arm stabilization has potential advantages and limitations. Co-contraction acts to stabilize the arm by activating antagonistic muscle pairs (Franklin et al. 2004). This mechanism is beneficial because it increases joint stiffness without the necessity for a complex motor control network to respond continuously to perturbations and appears to be the preferred method of stabilization when a dynamic force field is present (Franklin et al. 2003a, 2003b). Increasing the co-contraction of the arm during arm movements and postural maintenance tasks results in better movement accuracy and less positional error, respectively, providing increased stability to the limb during reach (Franklin et al. 2003a, 2003b; Gribble et al. 2003; Scheidt and Ghez 2007). A limitation of co-contraction for postural control of the arm is that it is thought to be metabolically inefficient (Gribble et al. 2003; Hogan 1984), because increased muscle activity is related to an increase in metabolic costs (Foley and Meyer 1993; Hogan et al. 1996; Sih and Stuhmiller 2003). Co-contraction is also only useful for perturbations that can be subdued by joint and musculature properties. The stiffness of the joint cannot exceed the physical properties of the tissues and tendons being used to stabilize the joint. Some joints, such as the ankle, have such low stiffness that they fall short of the of the minimum required for stability, which may also occur in the joints of the arm if strong perturbations are encountered (Hof 1998; Morasso and Sanguineti 2002; Morasso and Schieppati 1999).

The spinal/supraspinal reflex mechanism for stabilization works by tailoring the reflex responses of the motor system to resist perturbations to position (Kurtzer et al. 2008; Shemmell et al. 2009; Soechting et al. 1981). Both short-latency (~25 ms) and long-latency reflexes (40–100 ms) are observed in response to muscle stretch; reflex regulation may be beneficial for stabilization because of the speed of the correction and limited need for higher level processing (Crago et al. 1976; Marsden et al. 1983). Short-latency reflexes can modulate their response depending on the underlying muscle activity (Mortimer et al. 1981; Soechting et al. 1981), providing a generic response to muscle stretch that may not account for task context. On the other hand, long-latency reflex mechanisms can modulate their responses to muscle stretch and perturbations in a task-specific manner, acting as an intermediary between short-latency reflexes and volitional responses (Mutha et al. 2008; Pruszynski et al. 2008; Shemmell et al. 2009; Soechting et al. 1981). Although long-latency reflexes are able to modulate the direction and amplitude of their responses when prior knowledge of the task is known (Pruszynski et al. 2008), Mutha and colleagues (2008) showed that the amplitude modulation of long-latency reflexes is limited during movements with changing task goals. Modeling studies have suggested that the cyclic response of reflex activity coupled to a viscoelastic system could lead to unbounded amplification of an initial

perturbation and even resemble spastic clonus due to reflex delays (Baratta et al. 1998; Hidler and Rymer 1999). The absence of clonic activity during visuomotor control of arm posture suggests that reflex gains may be limited under normal circumstances, reducing this instability issue.

Cortically driven intermittent voluntary corrections could also provide visuomotor control of arm posture (Hasan 2005). Cortical involvement during stabilization can be beneficial due to the highly context-dependent responses generated as a result of the proprioceptive and visual information arriving at the cortex. However, cortically driven corrections of arm posture are limited by the long delays (150–200 ms) associated with sensory feedback and generation of corrective responses (Mutha et al. 2008; Pruszynski et al. 2008), as well as a larger computational load associated with the use of higher level motor control mechanisms to achieve stabilization goals without excessive cumulative errors. The lack of excessive error implies that prediction using some form of internal representation or model may be utilized for visuomotor control of arm posture (Shadmehr et al. 2010).

Co-contraction, spinal/supraspinal reflex, and cortically driven voluntary correction mechanisms of arm stabilization are not mutually exclusive and are most likely all employed during stabilization tasks. Experiments involving arm movement tasks have shown co-contraction decreases over time, possibly indicating a shift from a co-contraction mechanism, which provides greater accuracy in the absence of a fully formed internal model, toward internal representations of the movement and feedforward control after practice (Franklin et al. 2003b; Gribble et al. 2003). Co-contraction also shares a relationship with short-latency reflexes. In unstable environments, as the level of co-contraction increases, the magnitude of the reflex response also increases, suggesting both are used to compensate for perturbations (Akazawa et al. 1983; Soechting et al. 1981). Research investigating the disruption of cortical activity using transcranial magnetic stimulation or disconnect between the cortex and the spinal cord in the people with spinal cord injury have shown that reflex activity is lowered and the baseline level of co-contraction is increased, respectively, when cortical drive is reduced (Shemmell et al. 2009). When investigating balance of an inverted pendulum with the ankles, Loram and Lakie (2002) showed that stability requires not only intrinsic ankle stiffness but also anticipatory neural modulation of ankle torque. Furthermore, intersegmental interactions during brief force perturbations show electromyography (EMG) responses in segments downstream from the perturbed segment that exacerbate instead of resist perturbations (Koshland et al. 1991; Lacquaniti and Soechting 1984, 1986). It has been suggested that this unexpected response cannot be completely explained by reflex activity and may arise from a repertoire of voluntary movements (Koshland et al. 1991; Latash 2000). Although co-contraction and spinal/supraspinal reflex activity both contribute to stabilization, there also appears to be a cortical component. Hasan (2005) proposed that stability of a perturbed system is not guaranteed by continuous resistance but rather by later events, including voluntary corrections.

In this study, we set out to identify the cortical mechanisms of visuomotor control of arm posture. We collected EMG, kinematic, and EEG data across four different experimental tasks designed to differentiate potential stabilization mechanisms and determine which are involved in stabilization of arm posture. Our approach used a reach-and-hold paradigm to place the arm at a target position where the mechanisms of visuomotor control of arm posture were tested during the ensuing hold period. We used a position control task with minimal arm stabilization requirements, a co-contraction task with pure arm co-contraction, a voluntary task with pure volitional arm movement, and a perturbation task consisting of a force field in which participants were asked to stabilize their arm. EEG beta-band (13–26 Hz) power fluctuations during stabilization were used as indicators of brain activity associated with motor function (Pfurtscheller and Lopes da Silva 1999a, 1999b; Steriade et al. 1990), and the coherence between EEG electrodes was used to measure functional connectivity between cortical areas (Rappelsberger et al. 1993). We tested the hypothesis that cortical error correction networks contribute to arm stabilization. As a result of the involvement of co-contraction during stabilization of reach, we anticipated that perturbations during postural stabilization of the arm would show signs of increased EMG co-contraction. If cortical error correction networks are being utilized during stabilization, we would expect the cortical activity during visuomotor control of arm posture would mimic voluntary goal-directed movement. Furthermore, we postulated that invoking cortical visuomotor control networks would result in higher connectivity between the sensory regions interpreting the error and the motor regions correcting posture.

MATERIAL AND METHODS

Participant Population

A sample of 10 right-handed healthy participants (age 21–34 yr, 6 men) participated in the study. All participants gave written informed consent, and all procedures were approved by the Marquette University Institutional Review Board in accordance with the Declaration of Helsinki. Inclusion criteria required that the participants be healthy with no known neurological disease or injury.

Test Apparatus

The study was conducted using a custom-built mechanical linkage (Fig. 1A). The linkage constrained movement to the horizontal plane and provided measurements of end-point trajectory using optical encoders (Celesco Transducer Products, Chatsworth, CA; BEI Sensors, Goleta, CA) located at each joint. The device frame was constructed using 2.5-cm × 2.5-cm extruded aluminum (80/20, Columbia City, IN) and contained three rotational joints to allow unrestricted movement in the horizontal plane. While the participant was seated at the device, the forearm was secured to an ultra-high-molecular-weight polyethylene tray located at the end of the manipulandum. An overhead projector displayed hand position and target location on an opaque screen (80 cm × 60 cm) directly above the plane of hand motion. The

device was interfaced with LabVIEW (National Instruments, Austin, TX) to control the projector display, record (1-kHz sampling rate) kinematic data, and generate digital pulses used to synchronize the timing of movement and EMG/EEG data collection.
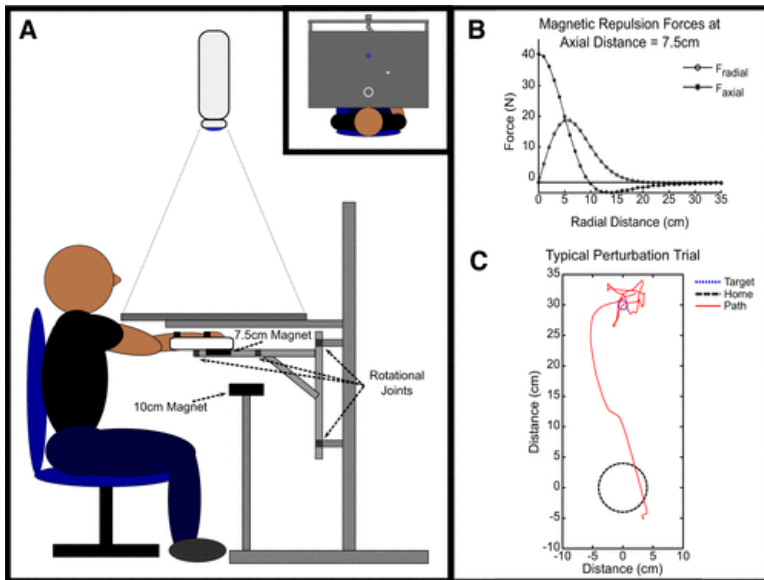

Fig. 1. *A*: illustration of the mechanical linkage and experimental setup from the side (*inset top right* displays the scene from above). The 10-cm diameter magnet was only present during the perturbation trials. The cursor (white circle) projected onto a horizontal screen was linked to hand position. Participants were required to move the cursor from the home location (gray annulus) to the target (blue annulus). *B*: magnetic repulsion forces in the radial and axial directions. The minimum axial distance between the magnets was 7.5 cm and occurred when the two magnets were directly over one another (radial distance = 0 cm). The maximum force in the radial direction of ~20.25 N was generated when the center of the 7.5-cm magnet was over the edge of the 10-cm magnet (~5 cm). *C*: typical perturbation trial. The time shown ranges from 0 to 6 s, from just after target presentation to the end of the stabilization period. The line represents the cursor's path (linked to hand position) throughout the trial. During the baseline period, the cursor (hand) slowly drifted out of the home location back toward the participant. Supplemental Video S1 (see https://doi.org/10.6084/m9.figshare.9199307) displays the typical perturbation trial.

Experimental Protocol

Before testing, EMG data were recorded from individual participants as they sat in a chair and performed maximum voluntary isometric contractions (MVCs) for the six muscles analyzed in this study. Each MVC was sustained for ~5 s. Anterior and posterior deltoid MVC data were collected as participants tried to internally or externally rotate the arm against resistance while the shoulder was abducted 90° in the plane of the scapula and the elbow was flexed 90°. Biceps and lateral head of the triceps MVC data were collected as participants tried to flex or extend the elbow against resistance while the shoulder was abducted 45° in the plane of the scapula and the elbow was flexed 90°. Flexor carpi radialis and extensor carpi ulnaris MVC data were collected as participants tried to flex and extend the wrist against resistance while

the shoulder was in a neutral position and the elbow was flexed 90°. These measurements were used later for normalization of EMG data obtained during the experimental trials.

The participant's dominant arm was tested using a period of stabilization following movements of the mechanical linkage. The study consisted of four tasks, each with 40 trials. Each trial consisted of a baseline period (6.5 ± 1.5 s before target presentation), target acquisition/stabilization period (0–6 s after target presentation), and return period (~1 s between the stabilization and baseline periods). Before each trial, participants were required to bring a white cursor (radius $r = 0.5$ cm), linked to hand position, to the home location (gray annulus, $r = 4$ cm) located ~24 cm in front of the participants. The home location then disappeared, and participants relaxed until the target (blue annulus, $r = 0.75$ cm) was presented 30 cm away from the home position on an imaginary line orthogonal to the participant's chest. Participants then moved their hand as quickly and accurately as possible to the target, at which point the four tasks began. The following tasks were tested.

Point-to-point task.

The point-to-point (PtP) task was designed to be a control task with minimal arm movements, EMG, co-contraction, and stabilization. After the point-to-point movement, participants were instructed to hold their hand at the target. The target and cursor were displayed for the duration of the target acquisition/stabilization period. No visual or physical perturbations were applied at the target.

Co-contraction task.

The co-contraction (CoC) task was designed to isolate the arm's EMG, co-contraction, cortical activity, and cortical connectivity associated with a pure co-contraction. After the point-to-point movement, participants were instructed to co-contract (10–20% of MVC) their arm at the target. Feedback regarding the level of co-contraction was given to the participants by way of cursor color (red, <10% deltoid MVC; white, within range; green, >20% deltoid MVC). Visual feedback of the target and cursor (level of co-contraction) was displayed for the first 2 s of the target acquisition/stabilization period, after which both were removed. Participants were instructed to hold the level of co-contraction constant after feedback was removed. No visual or physical perturbations were applied at the target.

Voluntary task.

The voluntary (VOL) task was designed to identify the EMG, co-contraction, cortical activity, and cortical connectivity associated with a volitional movement. After the point-to-point movement, participants were instructed to recreate the typical movement profile made when trying to stabilize their arm during the perturbation task (see below). This resulted in participants randomly moving their arm with approximately the same speed and within the same space that they did during the perturbation tasks. Visual feedback of the target was

displayed for the first 2 s during the target acquisition/stabilization period, after which it was removed. Participants continued to recreate movements similar to those of the perturbation task (see below) after the feedback was removed. No visual or physical perturbations were applied at the target.

Perturbation task.

The perturbation (PER) task was designed to generate EMG, co-contraction, cortical activity, and cortical connectivity associated with arm stabilization in an unstable environment. After the point-to-point movement, participants were instructed to keep the cursor on the target while axial and radial magnetic forces were applied at the target and the visual feedback was simultaneously manipulated to create a hyperbolic distortion of cursor position about the target. The magnetic force perturbation was created using two neodymium ring magnets (Applied Magnets, Plano, TX). The repulsive forces generated between the two magnets versus the distance of the hand away from the center of the target can be seen in Fig. 1*B*. The first magnet (diameter = 10 cm, thickness = 2.5 cm, center hole = 0.8 cm) was mounted under the screen target location, whereas the second (diameter = 7.5 cm, thickness = 1.2 cm, center hole = 0.8 cm) was mounted on the arm support tray under the hand. The minimum distance between the two magnets was 7.5 cm (Fig. 1*A*). Manipulation of visual feedback of arm position was generated using a hyperbolic function (*Eq. 1*), which changed the relationship between hand location and cursor location near the target,

$$X_C(X_H) = \begin{cases} \sqrt{-a^2[1 - (\frac{|X_H - X_T| + a}{a})^2]} + X_T; & \text{if } X_H \geq X_T \\ -\sqrt{-a^2[1 - (\frac{|X_H - X_T| + a}{a})^2]} + X_T; & \text{if } X_H < X_T \end{cases} \quad (1)$$

where X_C is the two-dimensional (2-D) cursor location, X_H is the 2-D hand location, X_T is the 2-D target location, and *a* represents the gain, which was randomly selected for each trial and varied between 5 ± 2.5 cm. Visual feedback was manipulated in the task to increase the sensitivity of hand movements around the target, effectively making the perturbation task more difficult. The visual gain was randomly selected each trial to prevent the participants from learning the perturbation environment. Figure 1*C* displays a typical perturbation trial time course.

The tasks were designed to compare the stabilization mechanisms active in the PER task with those in the CoC task (co-contraction mechanism during stabilization) and the VOL task (cortically driven voluntary correction mechanism during stabilization). Trials were blocked by task, with task presentation randomized across participants (the PER task always occurred before the VOL task to allow perturbation movement trajectories to be mimicked). Participants were given breaks between tasks to prevent fatigue.

Physiological Measurements

A 64-channel actiCAP active electrode system (Brain Products, Munich, Germany) arranged in the conventional 10–20 system with the reference at FCz and the ground at AFz was used to record EEG data. The EEG cap was placed on the participant's head such that the Cz electrode was in line with the prearticular points of the frontal plane and with the nasion and inion points of the sagittal plane. SuperVisc gel (Brain Products) was applied between the scalp and electrodes to lower the electrode impedances below 10 kΩ. EEG data were amplified, sampled at 1 kHz, filtered from 0.1 to 200 Hz, notch filtered at 60 Hz using a SynAmps 2 amplifier system (Neuroscan, Charlotte, NC), and recorded using the Neuroscan software Scan 4.5.

A Trigno wireless EMG system (Delsys, Boston, MA) recorded muscle activation from the anterior deltoid (AD), posterior deltoid (PD), flexor carpi radialis (WF), extensor carpi ulnaris (WE), biceps (BI), and lateral head of the triceps (TRI). The skin was cleaned and lightly abraded before electrodes were placed on the muscle. EMG data were amplified by 1,000 and sampled at 1 kHz.

Data Analysis

EEG data were post-processed and analyzed using the EEGLAB toolbox (version v13.4.4b) (Delorme and Makeig 2004), FieldTrip (version 2016-01-03) (Oostenveld et al. 2011), Brainstorm (version 3.4) (Tadel et al. 2011), and custom MATLAB scripts (version 2014a; The MathWorks, Natick, MA). All EEG data were bandpass filtered (0.1–100 Hz) using a fourth-order zero-phase Butterworth filter. The data were then epoched (−3 to 6 s relative to the movement cue) and baseline corrected (−3 s to cue). Bad epochs were removed (average number removed: 4) using EEGLAB's automatic rejection algorithm (200-μV threshold; pop_autorej) and manually by using FieldTrip's visual inspection code (epoch removed if its variance/kurtosis was a visual outlier compared with the other epoch variances/kurtoses for the task; ft_rejectvisual). EEG data were separated into signal and artifactual components using an adaptive mixture independent component analysis (AMICA) (Palmer et al. 2008), with 64 independent temporal components. Signal artifacts, including eye blink, EMG, and movement artifacts, were identified by distinct artifactual characteristics (Delorme et al. 2012; Makeig et al. 2004; Mognon et al. 2011; Puce and Hämäläinen 2017) and removed from the EEG data (average number of artifact components removed: 14; minimum number: 4; maximum number: 23). The remaining components were then transformed back to the EEG channel space. Finally, EEG data were re-referenced to a common average for all data analyses, excluding the connectivity analyses, which re-referenced the data to the average of the mastoids (electrodes TP9 and TP10) (Rappelsberger 1989). Each re-reference technique reintroduced the FCz electrode to the data set.

EMG data were processed and analyzed using custom MATLAB scripts (version 2014a; The MathWorks). All EMG data were bandpass filtered (10–350 Hz) using a fourth-order zero-

phase Butterworth filter and then sent through a root-mean-square (RMS) calculation using a 100-ms sliding window. To normalize the RMS EMG data from the experimental tasks, each muscle's RMS EMG trace was divided by its respective MVC value and multiplied by 100 to obtain the percentage of maximum voluntary EMG activation. Each muscle's MVC was calculated by finding the peak RMS EMG value within the muscle's MVC trial and taking the average of the surrounding 1-s window of time. EMG co-contraction was calculated at each sample point in time by taking the minimum normalized EMG activation from each agonist-antagonistic muscle pair (AD/PD, WF/WE, BI/TRI). Normalized EMG and EMG co-contraction data were epoched (−3 to 6 s relative to the movement cue), and bad epochs identified from the EEG data were removed. Normalized EMG and EMG co-contraction data were compared across tasks to characterize the contribution of co-contraction mechanisms to stabilize the arm during the PER task.

The speed of the hand was calculated from the x and y hand positions obtained from the optical encoders. Hand displacement was calculated as the Euclidean distance of the hand from the target. Speed and displacement data were both epoched (−3 to 6 s relative to the movement cue), and the bad epochs identified in the EEG data were removed. Hand displacement and speed were examined to ensure that the kinematics were matched between the PtP and CoC tasks as well as the VOL and PER tasks.

Distributed source localization was applied to the EEG data to examine the spatiotemporal characteristics of beta-band power (cortical activity) of the PER task and determine the cortical control mechanisms at play. Distributed current dipole maps were computed in Brainstorm using the default MNI/Colin27 anatomical brain template. The standard actiCAP electrode locations were fit to the scalp surface so that the Cz electrode location was at the vertex as described in *Physiological Measurements*. A boundary element model (BEM) was used to estimate of the forward model (OpenMEEG) (Gramfort et al. 2010; Kybic et al. 2005), and a depth-weighted minimum L2 norm estimator of cortical current density (Hämäläinen and Ilmoniemi 1994) was used to estimate the inverse model. The source localized data were then bandpass filtered (13–26 Hz) using a fourth-order zero-phase Butterworth filter, squared to obtain power, averaged across trials, low-pass filtered (2 Hz) using a fourth-order zero-phase Butterworth filter to extract the envelope, and normalized. For display purposes, the normalization process for the data shown in Fig. 3 was the Z score (baseline period: −3 s to cue). For statistical analyses, the normalization process was the calculation of the percent change from baseline (baseline period: −3 s to cue) (*Eq. 2*),

$$\%\Delta(t) = 100 \times \frac{X(t) - \text{baseline}}{\text{baseline}} \quad (2)$$

where $\%\Delta(t)$ represents the percent change from baseline, $\boldsymbol{X}(t)$ represents the power time series, t represents time, and *baseline* represents the average power in the baseline period.

EEG beta-band power of the source localization data was segmented into seven regions of interest (ROIs) using the Desikan–Killiany mapping technique (Desikan et al. 2006): left superior frontal gyrus, left caudal middle frontal gyrus, left precentral gyrus, left postcentral gyrus, left superior parietal gyrus, left inferior parietal gyrus, and left lateral occipital gyrus. The mean beta-band power for each of the seven ROIs was then compared across tasks. To examine hemispheric differences, an identical process was performed by treating the seven ROIs within each hemisphere as one large ROI and comparing the beta-band power mean difference between hemispheres.

EEG coherence was used to quantitatively compare cortical network connectivity between the PER task and the VOL (cortically driven mechanism) and CoC (co-contraction mechanism) tasks. All-to-all (connectivity between all possible pairs of EEG electrodes) temporal connectivity profiles were generated using magnitude squared coherence (*Eq. 3*),

$$\text{Coh}^2(f) = \frac{|C_{XY}(f)|^2}{C_{XX}(f) \cdot C_{YY}(f)} \quad (3)$$

where Coh^2 represents the magnitude squared coherence between electrodes X and Y, C_{XY} represents the cross spectrum between electrodes X and Y, C_{XX} represents the autospectrum of electrode X, C_{YY} represents the autospectrum of electrode Y, and f represents frequency. Every EEG epoch was divided into nine nonoverlapping windows, each containing 1 s of data. Coherence was then calculated within each window, using the epochs as the measure of consistency. For each participant and task, this resulted in a connectivity matrix that was 4,225 (65 × 65 electrodes) by 9 for every frequency. The resulting connectivity matrices were then averaged across the 13- to 26-Hz range and baseline corrected by removing the mean of the first three time points (representing the 3 s before the movement cue) to calculate task-based coherence of the beta-band. For each participant and task, a threshold was calculated by generating a histogram using the baseline-corrected connectivity values for all electrode-electrode combinations and finding the connectivity value corresponding to the top 5% of all connectivity values across the distribution. Connections that fell above the threshold were considered active.

EEG task-based coherence data were segmented into three ROIs: frontal cortex (electrodes Fp1, Fp2, AF7, AF3, AF4, and AF8), sensorimotor cortex (electrodes C3, C1, Cz, C2, C4, CP3, CP1, CPz, CP2, and CP4), and visual cortex (electrodes PO3, POz, PO4, O1, Oz, and O2). Intraregional and interregional coherence were then examined at each time point by calculating the percentage of active connections (PAC; *Eq. 4*) within each region and between each region, respectively,

$$\text{PAC} = 100 \times \frac{\#\text{Active}}{\#\text{Total}} \quad (4)$$

where # Active represents the number of connections above threshold and # Total represents the total number of connections.

Hand speed, hand distance, EMG activity, EMG co-contraction, EEG ROI beta-band power, EEG hemisphere beta-band power, EEG intraregional coherence, and EEG interregional coherence data were all averaged during the last 2 s (4–6 s) of the target acquisition/stabilization period (referred to as the stabilization period henceforth) and across trials for each participant. Although arm postural stabilization began immediately after the reach to the target, we chose to analyze the stabilization period 4–6 s after target presentation to minimize effects due to reach (~0.5–1.5 s after target presentation) and the removal of visual feedback (2 s after target presentation). Gwin and Ferris (2012) have shown that beta-band desynchronization can persist for ~1 s after the initial force generation in a sustained knee and ankle isometric task. Pfurtscheller and Lopes da Silva (1999b) recommend having ~10 s between events when studying EEG desynchronization to allow the frequency band modulations to recover. In our experience, beta-band modulations tend to stabilize between 1 and 10 s after movement. To prevent fatigue, we chose not to extend the period of stabilization analysis beyond 6 s, which resulted in our test period being 4–6 s after target presentation.

Statistical Analysis

To test our hypothesis that cortical error correction networks contribute to visuomotor control of arm posture, changes in EEG ROI beta-band power, EEG hemisphere beta-band power, EEG intraregional coherence, and EEG interregional coherence during the stabilization period were characterized across participants using repeated-measures two-way ANOVAs with task and space as factors in the analysis. Changes in EMG activity and EMG co-contraction during the stabilization period were characterized across participants using repeated-measures one-way MANOVAs (Pillai's trace) with task as the factor in the analysis; this allowed us to determine if co-contraction mechanisms were being utilized during the PER task. To ensure common kinematics between tasks, changes in hand speed and distance during the stabilization period were characterized across participants using repeated-measures one-way ANOVAs with task as the factor in the analysis. One-way ANOVAs were used as post hoc tests if any effects were found significant in the two-way ANOVAs or one-way MANOVAs. The Holm–Sidak method for correcting for multiple comparisons was used at each level (between multiple ANOVAs) in the analysis except for the pairwise comparisons, where Tukey's post hoc test was applied. When assumptions of the ANOVA were violated such as normality, a nonparametric bootstrap approach similar to the method of Zhou and Wong (2011) with 10,000 iterations was used to generate the statistical distributions for the two-way ANOVA, one-way ANOVA, and Tukey's post hoc tests. Statistical tests were performed with a type I error rate of $\alpha = 0.05$. All variables tested had at least one sample population that violated normality.

RESULTS

Movement Kinematics

Hand kinematics (displacement and speed) during the stabilization period were similar for the PtP and CoC tasks and for the VOL and PER tasks, with more movement and displacement occurring in the VOL and PER tasks. The one-way ANOVAs of hand displacement [$F(3,27) = 29.93$, $P < 0.0001$] and hand speed [$F(3,27) = 46.41$, $P < 0.0001$] during the stabilization period revealed significant differences among the tasks. The post hoc analysis (Tukey's test) of task differences for hand displacement and hand speed revealed that hand displacement [$q(27) > 8.62$, $P < 0.0001$] and hand speed [$q(27) > 10.25$, $P < 0.0001$] were significantly lower in the PtP and CoC tasks compared with the VOL and PER tasks. The lack of differences [hand displacement: $q(27) < 1.17$, $P > 0.848$; hand speed: $q(27) < 2.62$, $P > 0.27$] between the PtP [hand displacement: 0.24 cm (SD 0.06); hand speed: 0.22 cm/s (SD 0.08)] and CoC tasks [hand displacement: 0.37 cm (SD 0.13); hand speed: 0.38 cm/s (SD 0.17)] as well as the lack of differences between the VOL [hand displacement: 3.04 cm (SD 1.58); hand speed: 11.14 cm/s (SD 4.86)] and PER tasks [hand displacement: 2.73 cm (SD 0.85); hand speed: 8.96 cm/s (SD 2.61)] indicate that hand kinematics were similar within these task pairs during the stabilization period and suggest they did not play a role in the significant differences found in the other variables.

Muscle Activity

In general, the EMG activity during the stabilization period was similar across all muscles in the PtP and VOL tasks and in the CoC and PER tasks, with higher activity in the CoC and PER tasks (Fig. 2*A*). The one-way MANOVA of EMG activity during the stabilization period revealed a significant difference [$F(18,72) = 2.97$, $P = 0.001$] between tasks for the muscles. The post hoc one-way ANOVAs for tasks showed significant differences between tasks in each muscle [$F(3,27) > 2.81$, $P < 0.049$]. The post hoc analysis (Tukey's test) of task differences within each muscle revealed that activity in PD and BI muscles was significantly lower in the PtP and VOL tasks compared with the CoC and PER tasks [$q(27) > 3.87$, $P < 0.0361$], activity in the TRI and WE muscles was significantly higher in the CoC task compared with the PtP and VOL tasks [$q(27) > 5.15$, $P < 0.0041$], activity in the WF was significantly lower in the PtP task compared with the CoC task [$q(27) = 4.73$, $P = 0.012$] whereas the activity in the WF was significantly higher in the PER task compared with the PtP, CoC, and VOL tasks [$q(27) > 4.55$, $P < 0.018$], and the activity in the AD did not result in any significant differences across tasks. The similarity in muscle activation between the PER and CoC tasks and the differences between the PER task and the PtP and VOL tasks indicate that more muscle activity was needed to position the arm during a stabilization (PER) task than is normally generated in a volitional arm movement (VOL) task, and that the level of muscle activity in an arm stabilization (PER) task resembles that seen in an arm co-contraction (CoC) task.
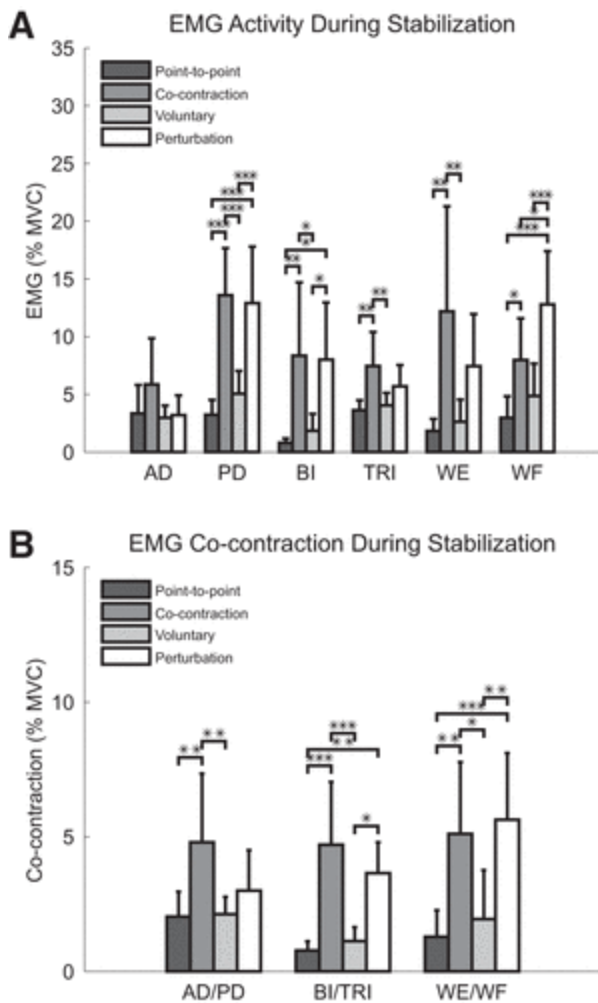
Fig. 2. *A*: electromyographic (EMG) activity during the stabilization period. *B*: co-contraction during the stabilization period. Muscles examined were the anterior deltoid (AD), posterior deltoid (PD), flexor carpi radialis (WF), extensor carpi ulnaris (WE), biceps (BI), and lateral head of the triceps (TRI). Both EMG activity and co-contraction were normalized to the respective muscle's maximum voluntary contraction (MVC). Values are %MVC averaged across all participants ($n = 10$, 6 men) with error bars denoting the 95% confidence interval about the mean. $*P < 0.05$; $**P < 0.01$; $***P < 0.001$, significant differences determined via post hoc analysis (Tukey's test).

Muscle Co-contraction

EMG co-contraction during the stabilization period was similar across all muscle pairs in the PtP and VOL tasks, with their EMG co-contraction being lower than in the CoC and PER tasks (Fig. 2*B*). The CoC and PER tasks had similar EMG co-contraction in the BI/TRI and WE/WF muscle pairs with a trend toward a significant difference in the AD/PD muscle pair. The one-way MANOVA of EMG co-contraction during the stabilization period revealed significant differences [$F(9,81) = 6.84$, $P < 0.0001$] between tasks for antagonistic muscle pairs. The post hoc one-way ANOVAs for tasks showed differences between tasks in each muscle pair [$F(3,27) > 6.51$, $P < 0.0015$]. The post hoc analysis (Tukey's test) on task differences within each muscle pair indicated that co-contraction in the BI/TRI and WE/WF pairs was significantly

lower in the PtP and VOL tasks compared with the CoC and PER tasks [$q(27) > 4.62$, $P <$ 0.0138] and that co-contraction in the AD/PD pair was significantly higher in the CoC task compared with the PtP and VOL tasks [$q(27) > 5.33$, $P < 0.0028$], with evidence for the co-contraction in the AD/PD pair being higher in the CoC task compared with the PER task [$q(27) = 3.58$, $P = 0.066$]. The similarity in muscle co-contraction between the PER and CoC tasks and the differences between the PER task with the PtP and VOL tasks indicate that more muscle co-contraction was used to position the arm in the stabilization (PER) task, whereas minimal muscle co-contraction was used in the control (PtP) and volitional arm movement (VOL) tasks.

Beta-Band Spatiotemporal Power

EEG beta-band power was examined to identify the time course of task-related activity across the cortex (decrease in beta-band power from baseline) and to determine if the cortical activity during a stabilization (PER) task resembled that of volitional control (VOL), co-contraction (CoC) tasks, or neither. A decrease in beta-band power relative to baseline was identified in premotor, motor, sensory, and parietal cortices and was located bilaterally in all tasks, as shown in Fig. 3. Source localization revealed that the spatiotemporal patterns of beta-band power decrease were similar between the PtP and CoC tasks and the VOL and PER tasks, respectively. The time course of activity for the PtP and CoC tasks had a transient desynchronization during movement onset, followed by a return to baseline power levels during the stabilization period. In contrast, beta-band desynchronization was sustained throughout the movement and stabilization periods for the VOL and PER tasks. The spatial extent of decrease in beta-band power during the initial reaching movement was slightly more extensive during the reach period for the VOL and PER tasks than for the PtP and CoC tasks, possibly indicating differences in planned motor commands due to the experimental block design. Similarities in spatiotemporal EEG beta-band power between the PER and VOL tasks and the differences between the PER task compared with the PtP and CoC tasks indicate that cortical networks used to control the arm during the stabilization (PER) task share areas and levels of activation similar to those involved in volitional arm movements (VOL), whereas minimal cortical network activity is associated with stabilization via arm co-contraction (CoC).
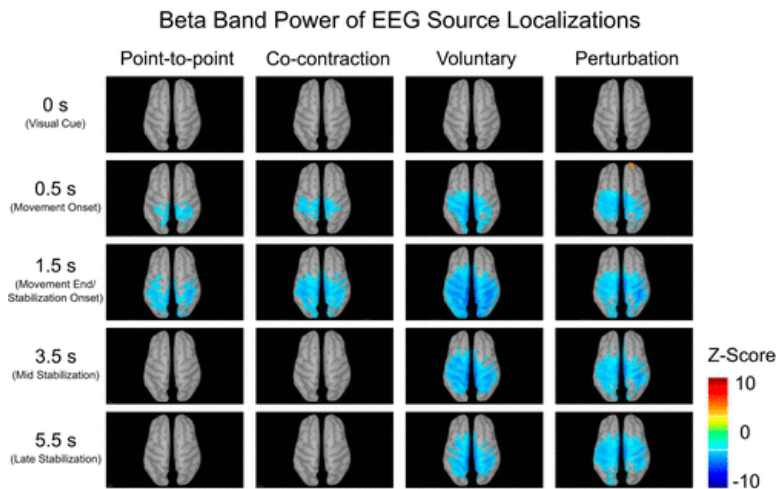
Fig. 3. EEG source localization of beta-band power. The Z score averaged across participants ($n = 10$, 6 men) is shown for each task. Each brain image shows a snapshot of a key time point taken from the continuous activity time course averaged across all participants. Only values above or below a Z-score threshold of ±3 are displayed. Negative values indicate beta-band desynchronization, whereas positive values indicate a resynchronization. The left hemisphere in each plot represents the hemisphere contralateral to the arm (dominant) tested.

Beta-Band Hemisphere Power

The EEG beta-band power during the stabilization period was lateralized, with the left (contralateral) hemisphere having more beta-band desynchronization, as shown in Fig. 4C. The VOL and PER tasks had similar activity, as did the PtP and CoC tasks, with the VOL and PER tasks' activity being higher (Fig. 4D). The two-way ANOVA of beta-band hemisphere power during the stabilization period showed no interaction effect but revealed a main effect of task [$F(3,27) = 14.51$, $P < 0.0001$] and hemisphere [$F(1,9) = 9.32$, $P = 0.012$]. The post hoc analysis (Tukey's test) of task differences indicated that the decrease in power was significantly lower in the PtP and CoC tasks compared with the VOL and PER tasks [$q(27) > 5.12$, $P < 0.008$]. The analysis of hemispheric EEG beta-band power demonstrated similar patterns of hemispheric activation across all four tasks, although the PtP and CoC tasks activated the pattern to a lower degree than the VOL and PER tasks. This could indicate an increased computational load during volitional movement generation (VOL) and stabilization (PER) of the arm compared with a control (PtP) and arm co-contraction (CoC) task.
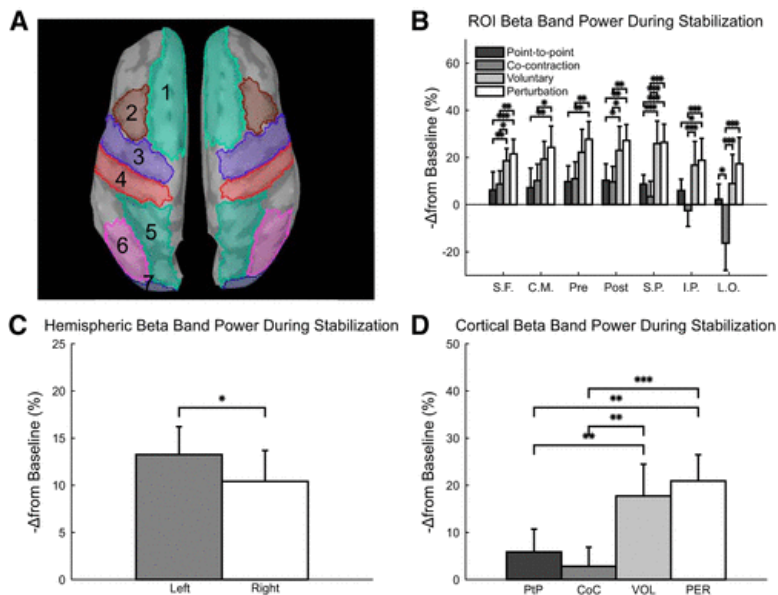
Fig. 4. *A*: brain with 7 regions of interest (ROIs) examined: *1*, left superior frontal gyrus (SF), *2*, left caudal middle frontal gyrus (CM); *3*, left precentral gyrus (Pre); *4*, left postcentral gyrus (Post); *5*, left superior parietal gyrus (SP); *6*, left inferior parietal gyrus (IP); and *7*, left lateral occipital gyrus (LO). *B*: ROI beta-band power during the stabilization period for the left hemisphere (contralateral to tested arm). *C*: hemispheric beta-band power during the stabilization period. *D*: cortical beta-band power during the stabilization period, an average of 14 ROIs (7 from each hemisphere). Values are %change in beta-band power from baseline ($-\Delta$ from baseline) averaged across participants ($n = 10$, 6 men) with error bars denoting the 95% confidence interval about the mean. *$P < 0.05$; **$P < 0.01$; ***$P < 0.001$, significant differences determined via post hoc analysis (*B* and *D*, Tukey's test; *C*, 2-way ANOVA main effect.

Beta-Band ROI Power

In general, beta-band power during the stabilization period was similar across all ROIs in the VOL and PER tasks with a larger decrease in beta-band power than in the PtP and CoC tasks, as shown in Fig. 4*B*. The PtP and CoC tasks had similar beta-band power in all ROIs except for the lateral occipital gyrus, where the CoC task showed a resynchronization of beta-band power. The two-way ANOVA of ROI beta-band power during the stabilization period revealed a main effect of task [$F(3,27) = 13.2$, $P < 0.0001$], a main effect of ROI [$F(6,54) = 6.97$, $P < 0.0001$], and an interaction effect between task and ROI [$F(18,162) = 3.82$, $P < 0.0001$]. The post hoc one-way ANOVAs for task showed differences between tasks in all ROIs [$F(3,27) > 5.12$, $P < 0.0058$]. The post hoc analysis (Tukey's test) of task differences within each ROI indicated that the decrease in power in the superior frontal, postcentral, and superior parietal gyri was significantly lower in the PtP and CoC tasks compared with the VOL and PER tasks [$q(27) > 4.12$, $P < 0.038$], the decrease in power in the caudal middle frontal and precentral gyri was significantly higher in the PER task compared with the PtP and CoC tasks [$q(27) > 4.03$, $P < 0.0358$], the decrease in power in the inferior parietal gyrus was significantly higher in the PER task compared with the PtP and CoC tasks [$q(27) > 4.26$, $P < 0.0293$] and was significantly higher in the VOL task compared with the CoC task [$q(27) = 6.44$, $P = 0.008$], and the decrease in power in the lateral occipital gyrus was significantly lower in the CoC task

compared with the PtP, VOL, and PER tasks [$q(27) > 4.69$, $P < 0.0123$]. Similarities in ROI EEG beta-band power between the PER and VOL tasks and the differences between the PER task compared with the PtP and CoC tasks indicate that similar cortical areas with levels of activation similar to those involved in volitional arm movements (VOL) were used to control the arm in the stabilization (PER) task. Meanwhile, arm co-contraction (CoC) had minimal activation across ROIs and even inhibited cortical activation (negative beta-band power) in the posterior ROIs.

Beta-Band Electrode Coherence

EEG beta-band coherence was examined to identify the cortical areas that were functionally connected during the tasks, to determine how their interactions evolved over time, and to compare the connectivity during stabilization for the task conditions (PER, VOL, CoC, PtP). Task-based coherence maps for electrode C3 (electrode over the sensorimotor cortex associated with the task) and for all electrode combinations during each task are shown in Figs. 5 and 6, respectively. Every coherence head map for electrode C3 had a similar pattern of coherence, with the highest task-based coherence occurring around the mirrored electrode (C4) in the opposite hemisphere and the lowest task-based coherence concentrated in the area around electrode C3. Patterns of task-based coherence were similar between the PtP and CoC tasks and the VOL and PER tasks, respectively. The temporal profile of the PtP and CoC tasks had a transient increase in coherence during movement onset and early stabilization, followed by a return to near baseline levels during late stabilization. In contrast, an increase in coherence was sustained throughout the movement and stabilization periods for the VOL and PER tasks. Even though the temporal patterns of task-based coherence were similar between the VOL and PER tasks, the PER task had much higher levels of coherence throughout electrodes that extended into the occipital areas. All-to-all coherence maps (maps of coherence between an electrode and all other electrodes) indicate that the PER task had more active connections at each time point and that the connections had a larger increase in coherence than the other three tasks. Similarities in EEG beta-band coherence between the PER and VOL tasks and the differences between the PER task compared with the PtP and CoC tasks indicate that the cortical networks used in an arm stabilization (PER) task share task-based functional connectivity patterns similar to those involved in volitional arm movements (VOL), whereas minimal task-based functional connectivity seemed to be involved with arm co-contraction (CoC). The fewer functional connections to visual regions during the arm co-contraction (CoC) and volitional arm movement (VOL) tasks compared with the arm stabilization (PER) task point to the increased role visual information played in the arm stabilization (PER) task.
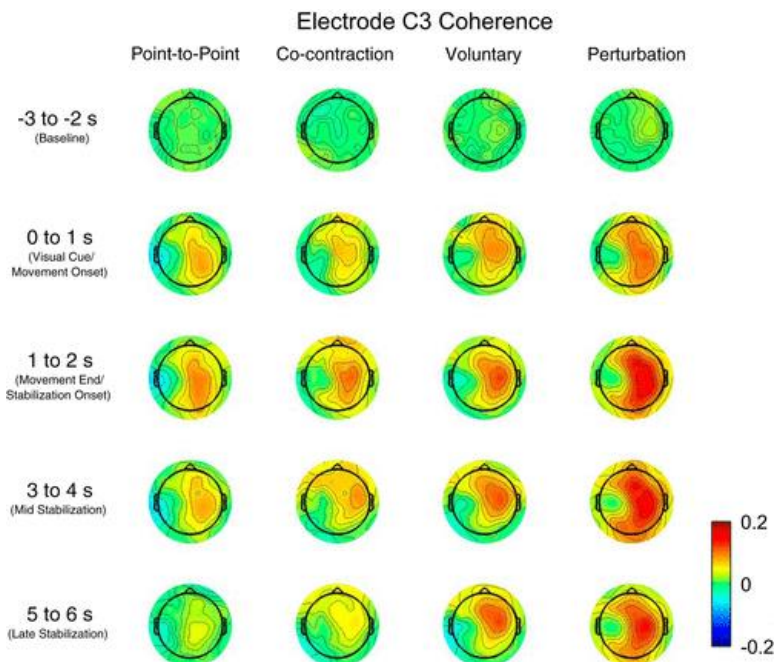
Electrode C3 Coherence

Fig. 5. Electrode C3 (left motor cortex) task-based coherence maps within the beta-band. The task-based coherence (coherence change from baseline period) averaged across participants ($n = 10$, 6 men) is shown for each task. Each head plot corresponds to a 1-s coherence window displaying key time ranges of the movement that indicate how electrode C3's task-based coherence varied spatially with different electrodes. Values of coherence were interpolated between electrodes. Negative values indicate a decrease in coherence, whereas positive values indicate an increase in coherence relative to the baseline period. The left hemisphere of each plot represents the hemisphere contralateral to the arm (dominant) tested.

All-to-All Electrode Coherence
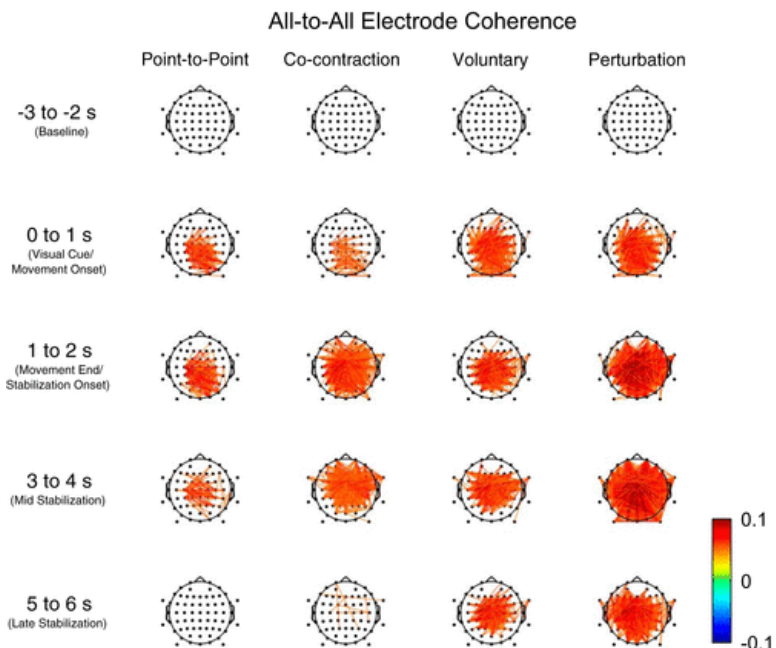
Fig. 6. All-to-all coherence maps of connectivity within the beta-band. Task-based coherence (relative to the baseline period) averaged across participants ($n = 10$, 6 men) is shown for each task. Each head plot corresponds to a 1-s coherence window displaying a key time range during the movement period and indicates the degree of functional connectivity between all pairs of electrodes. Only values above or below a task-based coherence threshold of ±0.05 are displayed, corresponding to the top 5% of coherence values observed during the baseline period. For each task, the threshold was calculated by

generating a histogram of the baseline period task-based coherence values averaged across participants for all electrode-electrode combinations and finding the coherence value at which only 5% of all coherence values fell above. Negative values indicate a decrease in coherence, whereas positive values indicate an increase in coherence relative to baseline. The left hemisphere in each plot represents the hemisphere contralateral to the arm (dominant) tested.

## Beta-Band Intraregional Coherence

The intraregional task-based coherence during the stabilization period was similar in the frontal and visual regions for all tasks (Fig. 7A). The sensorimotor region showed differences between the PER task and the PtP and CoC tasks, whereas the PtP and CoC tasks and the VOL and PER tasks had similar task-based coherence during the stabilization period. The two-way ANOVA of intraregional task-based coherence during the stabilization period revealed a main effect of task [$F(3,27) = 2.90$, $P = 0.049$], a main effect of region [$F(2,18) = 13.52$, $P = 0.0005$] and an interaction effect between task and region [$F(6,54) = 3.42$, $P = 0.0062$]. The post hoc one-way ANOVAs for tasks showed differences between tasks in the sensorimotor region [$F(3,27) = 7.04$, $P = 0.0018$]. The post hoc analysis (Tukey's test) of task differences within the sensorimotor region indicated that the coherence was significantly higher in the PER task compared with the PtP and CoC tasks [$q(27) > 4.91$, $P < 0.0091$]. The similarities in intraregional task-based coherence in the frontal and visual regions indicate comparable levels of communication in these regions across tasks. The similar intraregional task-based coherence in the sensorimotor region between the PER and VOL tasks and the higher task-based connectivity in the PER task compared with the PtP and CoC tasks indicate that the sensorimotor networks used in an arm stabilization (PER) task shared task-based functional connectivity patterns similar to those involved in volitional movements, and they tended to be larger than those found in the co-contraction (CoC) task.
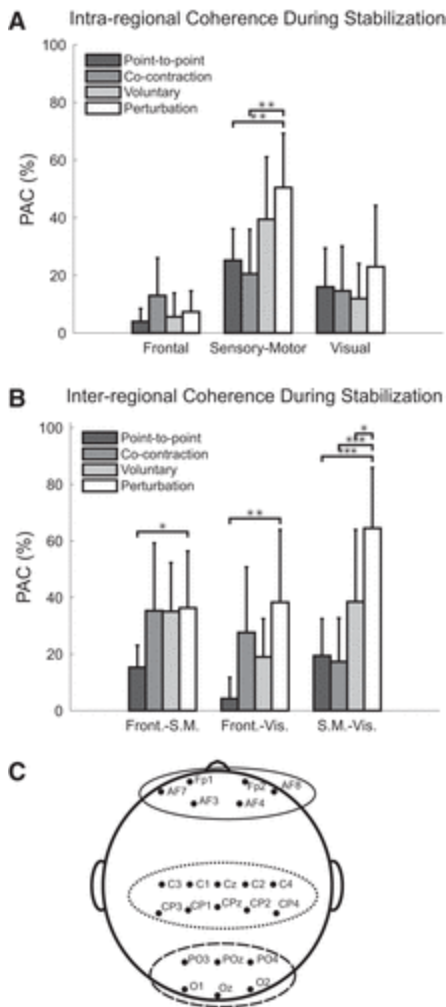
Fig. 7. *A*: intraregional beta-band coherence during the stabilization period. *B*: interregional beta-band coherence during the stabilization period. *C*: EEG electrode head map with electrode groups identified with circles. Solid circle, frontal cortex (Front.) electrodes Fp1, Fp2, AF7, AF3, AF4, and AF8; dotted circle, sensorimotor cortex (S.M.) electrodes C3, C1, Cz, C2, C4, CP3, CP1, CPz, CP2, and CP4); dashed circle, visual cortex (Vis.) electrodes PO3, POz, PO4, O1, Oz, and O2. Values are the beta-band percentage of active connections (PAC) averaged across participants ($n = 10$, 6 men) with error bars denoting the 95% confidence interval about the mean. $*P < 0.05$; $**P < 0.01$; $***P < 0.001$, significant differences determined via post hoc analysis (Tukey's test).

Beta-Band Interregional Coherence

The interregional task-based coherence during the stabilization period was similar for all region pairs for the PtP, CoC and VOL tasks (Fig. 7*B*). The sensorimotor/visual region pair showed higher levels of task-based coherence in the PER task compared with all other tasks. The two-way ANOVA of interregional task-based coherence during the stabilization period revealed a main effect of task [$F_{(3,27)} = 7.60$, $P = 0.003$], a main effect of region pairs [$F_{(2,18)} = 3.97$, $P = 0.039$] and an interaction effect between task and region pairs [$F_{(6,54)} = 4.70$, $P < 0.0001$]. The post hoc one-way ANOVAs for tasks showed differences between tasks in all region pairs [$F_{(3,27)} > 3.43$, $P < 0.0299$]. The post hoc analysis (Tukey's test) of task differences within region pairs indicated that the coherence in the frontal/visual and the frontal/sensorimotor

region pairs was significantly lower in the PtP task compared with the PER task [$q(27) >$ 5.13, $P < 0.0475$] that and the coherence in the sensorimotor/visual region pair was significantly higher in the PER task compared with the PtP, CoC, and VOL tasks [$q(27) >$ 3.89, $P < 0.048$]. The increase in interregional task-based coherence of the sensorimotor/visual region pair for the PER task compared with the PtP, CoC, and VOL tasks suggested an increased reliance of sensorimotor processing on visual information during an arm stabilization (PER) task compared with an arm co-contraction (CoC) or volitional arm movement (VOL) task.

DISCUSSION

Main Results

In this study, we set out to identify the cortical mechanisms involved in arm stabilization and to test the hypothesis that cortical error correction networks contribute to visuomotor control of arm posture. This study demonstrated that visuomotor control of arm posture involves co-contraction of antagonistic muscles as well as cortical networks with increased connectivity between pathways associated with error correction. Specifically, during the stabilization period, cortical activity (reduction in EEG beta-band power from baseline) in the PER task was comparable to that in the VOL task and did not resemble the activity seen in the PtP or CoC task (Figs. 3, 4*B*, and 4*D*). The cortical networks identified during arm stabilization resembled those seen in volitional arm movement generation, suggesting volitional corrections may be one of the strategies the brain uses to stabilize the arm. The level of network connectivity (change in EEG beta-band coherence from baseline) between the sensorimotor and visual regions was higher in the PER task compared with the PtP, CoC, and VOL tasks (Fig. 6*B*). Increased connectivity between the sensorimotor and visual regions suggests visual feedback of error to the motor cortex for the generation of corrective movements. Stiffening of the arm via co-contraction of antagonistic muscle pairs was higher during the PER task compared with the PtP and VOL tasks (Fig. 2), suggesting co-contraction mechanisms were also employed during stabilization of the arm. The presence of high cortical activity that resembled volitional motor generation and high connectivity in error pathways only seen in the stabilization (PER) task indicates the involvement of cortical mechanisms in postural control of the arm that are distinct from short-latency impedance control of the arm via activation of antagonistic muscles and spinal/supraspinal reflex activity. Cortical networks encompassing sensory, motor, and visual areas appear to play an important role in stabilization of arm posture.

Role of the Cortex in Visuomotor Control of Arm Posture

The comparable levels of cortical activation found between the VOL and PER tasks suggests that the brain may be using similar control mechanisms in both tasks. This similarity in cortical activity may arise from mapping the changes in limb position and/or from motor commands generated during the tasks. Although passive movements of the upper limb have been found

to activate similar cortical areas as active movements, the level of activation tends to be less (Formaggio et al. 2013; Guzzetta et al. 2007; Weiller et al. 1996). Furthermore, isometric force generation (Gwin and Ferris 2012) and voluntary movements under ischemic nerve block conditions (Christensen et al. 2007) have been shown to involve cortical activation, indicating that motor output as well as sensory feedback/processing is associated with cortical activity. Although it is difficult to distinguish motor output from sensory feedback/processing, the need to identify visual changes in arm position from the target in the PER task suggests the observed brain activity reflects the processing of sensory feedback in addition to generating volitional commands to stabilize the arm.

Measures of cortical coherence suggest that widespread cortical networks play an important role in arm stabilization. During the PER task, connectivity between the visual and sensorimotor networks was higher than during the other tasks, suggesting the transfer of visual information to sensorimotor cortices (Fig. 7B). Because the VOL task is also a visuomotor task, we expected a similar network to the PER task, but to a lesser degree due to the lower task relevance of visual information and the lack of an error signal. Although not significantly different, the connectivity between the sensorimotor and visual regions was larger for the VOL task compared with the PtP and CoC tasks (Fig. 7B; $P < 0.067$). Since the movement kinematics and sensory information were similar between the VOL and PER tasks, the PER task's increase in connectivity between the sensorimotor and visual regions suggests the recruitment a visual error network. Similar sensorimotor/visual networks have been reported in studies involving finger and wrist movements where the frontal lobe, sensory cortex, motor cortex, parietal cortex, and occipital lobe have been shown to function together to control movement (Chen et al. 2003; O'Neill et al. 2017; Sukerkar 2010). These findings provide support for Hasan's hypothesis that cortically driven intermittent voluntary corrections provide stability to arm posture (Hasan 2005).

Although the results support the involvement of a cortically mediated error network during arm stabilization, it is impossible to rule out the influence of spinal/supraspinal reflex circuitry on the observed cortical activation. Ideally, the study would have included metrics to quantify all three proposed mechanisms of arm stabilization: 1) increased impedance of the arm through the co-contraction of antagonistic muscles (Franklin et al. 2004), 2) spinal or supraspinal reflex circuits to provide corrective muscle activity (Kurtzer et al. 2008), and 3) intermittent voluntary corrections to errors in position (Hasan 2005). Long-latency, supraspinal reflex activity is cortically modulated, generates cortical activity, and can be task dependent (Abbruzzese et al. 1985; Cheney and Fetz 1984; Pruszynski et al. 2008, 2011a, 2011b; Shemmell et al. 2009). Long-latency reflexes also have the capacity to incorporate feedback from the task and modulate activity at the cortical level in a fashion similar to volitional movements (Mutha et al. 2008; Pruszynski et al. 2011a, 2011b). However, the cortical activity associated with long-latency reflexes is not as extensive as volitional movements (Suminski et al. 2007). Previous EEG research investigating long-latency reflexes and volitional responses suggests different cortical mechanisms for each response based on differences in the EEG topographies (Spieser et al. 2010). One study suggests that long-latency reflexes are associated with

different visual pathways than voluntary corrections (Mutha et al. 2008), whereas another has even suggested that long-latency mechanisms, postural stability, and instructed reaction use different neural pathways (Shemmell et al. 2009). Furthermore, long-latency reflex activity is still present in spinalized cats and monkeys (Ghez and Shinoda 1978; Tracey et al. 1980), raising questions about whether supraspinal structures are directly involved in the reflex response. Spinal turtles can generate a scratch reflex (Stein and Grossman 1980), and spinal frogs show stability of limb targeted movements (Pfluger 1853), suggesting, at least in lower vertebrates, that reflexes and stability are still possible without cortical input. Thus, although the cortex may play a role in modulating long-latency reflex activity, the associated cortical component/activity may differ from volitional control, and the mechanism of generation may lie within the spinal system.

Stabilization Mechanisms

The use of co-contraction, spinal/supraspinal reflex, and cortically driven voluntary correction mechanisms of postural control are not mutually exclusive and are likely all employed during arm stabilization tasks. We found increased levels of arm co-contraction in our stabilization (PER) task similar to that found in the pure co-contraction (CoC) task, indicating increased impedance of the arm through co-contraction of antagonistic muscles (Franklin et al. 2004). This result is consistent with previous research showing increased co-contraction of the arm provides stability to the limb (Franklin et al. 2003a, 2003b; Gribble et al. 2003; Scheidt and Ghez 2007). Although arm co-contraction is utilized, the minimal cortical activity in the CoC task compared with the extensive cortical activity in the PER task suggests that co-contraction is not the only active stabilization mechanism. Though not explicitly tested for in this study, spinal and supraspinal reflex circuits (Kurtzer et al. 2008) are likely also present during the PER task, since both short-latency (~25 ms) and long-latency reflexes (40–100 ms) are observed in response to muscle stretch (Crago et al. 1976; Marsden et al. 1983). However, the cortically mediated error network identified in the PER task most likely reflects voluntary corrections to errors in position (Hasan 2005).

Co-contraction, reflex control, and voluntary corrections probably work in concert to provide stabilization after a reach. Co-contraction works to stabilize the limb when forces can be subdued with physical properties of the tissues at the joint (Franklin et al. 2003a, 2003b). If the mechanical properties of the joint cannot provide the required stiffness for stability, reflex activity could increase stability. When reflex activity fails to produce stability or a more dynamic mode of stability is required (Mutha et al. 2008), cortically driven voluntary corrections may be used (Hasan 2005). In line with this idea, ankle and wrist stability requires not only intrinsic stiffness and reflex activity but also modulations of joint torque (Loram and Lakie 2002; Suminski et al. 2007).

Although this study focused on increased impedance of the arm through the co-contraction of antagonistic muscles (Franklin et al. 2004), spinal or supraspinal reflex circuits to provide corrective muscle activity (Kurtzer et al. 2008), and intermittent voluntary corrections to errors

in position (Hasan 2005), other potential stabilization mechanisms are possible. For example, fractional power damping, in which ongoing joint movements are braked by stretch reflexes in the antagonistic muscle, could also be used to stabilize the limb (Houk et al. 2000). In fractional power damping, motor commands are used to tune the stretch reflex thresholds, which sets a new equilibrium point of the joint. This model of antagonistic reflex activation around an equilibrium point results in a damped system with no oscillations. The fractional power damping model is limited in that it only describes an open-loop process with respect to setting the equilibrium point. A complete model would also need to include visual feedback to generate accurate motor commands in the presence of error.

Bilateral Hemispheric Activation with Lateralization

EEG beta-band power revealed extensive bilateral desynchronization during the stabilization phase of movement (Fig. 3). Active areas of the cortex included but were not limited to the superior frontal, caudal middle frontal, precentral, postcentral, superior parietal, inferior parietal, and lateral occipital gyri. Previous EEG studies examining voluntary thumb, finger, hand, and foot movements have reported event-related desynchronization that is localized bilaterally near sensorimotor homunculi associated with the active muscle groups (Pfurtscheller et al. 1997, 1999; Pfurtscheller and Lopes da Silva 1999b). During movements of the entire arm, a larger portion of the cortex undergoes event-related desynchronization, suggesting that the number of muscle groups activated affects event-related desynchronization (Pfurtscheller et al. 1999). In addition, Pfurtscheller and colleagues (1994) have shown that visual and parietal areas exhibit event-related desynchronization during a visual processing task. In this study, muscle groups of the entire arm were active during a more complicated end-point visuomotor stabilization task, which may have contributed to the extensive cortical activation.

In addition to the extensive bilateral activation during visuomotor control of arm posture, the contralateral hemisphere was significantly more active than the ipsilateral hemisphere (Fig. 4). This observation supports previous EEG and fMRI studies examining hand movements, which consistently show bilateral cortical activity to be more pronounced on the contralateral hemisphere (Formaggio et al. 2013; McFarland et al. 2000; Yuan et al. 2010). Even though the lateralization of cortical activity to the contralateral hemisphere is expected, there was little interaction between task and hemisphere associated with a "dynamic dominance" mechanism (Sainburg 2002, 2005), in which the dominant limb/hemisphere is specialized for coordination and the nondominant limb/hemisphere is specialized for stabilization. The dynamic dominance hypothesis would predict that the cortical activity in the PtP, CoC, and PER tasks (end-point stabilization processes) would be lateralized to the ipsilateral (nondominant) hemisphere, whereas the cortical activity in the VOL task (trajectory control processes) would be lateralized to the contralateral (dominant) hemisphere. Although cortical activity was lateralized to the contralateral hemisphere, both trajectory control (VOL) and end-point stabilization (PtP, CoC, and PER) tasks also showed ipsilateral activation.

Decrease of Cortical Activity During Co-contraction

An interesting finding was the lack of a sustained beta-band desynchronization during the stabilization period of the CoC task (Figs. 3 and 4*B*). The lack of cortical activity occurred despite EMG activity at similar levels as the PER task (Fig. 1*A*). The only notable differences in the CoC and PER tasks during the stabilization period were that the hand was moving during the PER task [hand speed: 8.96 cm/s (SD 2.61)] with the target still visible, whereas the hand was stationary [hand speed: 0.38 cm/s (SD 0.17)] with no visual feedback of the target in the CoC task. The lack of cortical activity during the sustained contraction is not unique to this study and has been documented in sustained wrist contractions and isometric contractions of the lower limb (Alegre et al. 2003; Gwin and Ferris 2012).

One possible explanation for the reduction in cortical activity is that activity associated with sensory feedback is large compared with the actual generation of motor commands (Weiller et al. 1996). Muscle and skin afferents provide feedback of proprioception at the cortical level, evidenced by EEG-evoked responses from imposed joint movements (Kornhuber and Deecke 2016) or nerve stimulation (Dawson 1947; Giblin 1964). Although the static proprioceptive feedback was similar across all tasks, movements of the limb during PER and VOL tasks could have triggered sensory EEG signals that differentiated the EEG patterns from CoC and PtP tasks. EEG and fMRI studies report similar areas of the cortical activation with slightly lower activation in passive vs. active movements (Formaggio et al. 2013; Guzzetta et al. 2007; Weiller et al. 1996). Beta desynchronization associated with joint movement is reduced in stroke survivors with pure somatosensory deficits (Platz et al. 2000) or when sensory feedback is muted by prolonged vibration (Lee and Schmit 2018). Although sensory feedback/processing does seem to play a large role in cortical activation associated with the control of movement, imagined hand movements (Formaggio et al. 2013; McFarland et al. 2000), attempted movements in people with spinal cord injury (Gourab and Schmit 2010), isometric force generation of the lower extremity (Gwin and Ferris 2012), and voluntary movements under ischemic nerve block conditions (Christensen et al. 2007) produce cortical activation, suggesting that proprioceptive feedback is only one driver of cortical activity in motor tasks.

Another possible explanation for the lack of cortical activity during CoC arises from the concept that beta-band activity corresponds to an idling rhythm in the motor system that maintains the current state (Engel and Fries 2010; Pfurtscheller and Lopes da Silva 1999b). Evidence for the maintenance of the current motor state comes from observations of impaired motor performance during naturally or artificially enhanced levels of beta-band activity, suggesting that the increased beta-band activity prevents the motor system from making dynamic changes (Gilbertson et al. 2005; Pogosyan et al. 2009). This is supported by Swann and colleagues (2009), who showed that successful stop trial performance in a Go/No-Go task is associated with enhanced beta-band activity.

Finally, the lack of cortical activity seen during sustained co-contraction may be because co-contraction mechanisms are relegated to the spinal level. After a spinal cord injury, humans have been shown to have altered upper extremity reaching movements (Wierzbicka and Wiegner 1992, 1996). In connection with this, Cremoux and colleagues (2017) have shown that co-contraction increases after a spinal cord injury, possibly due to reduced cortical influence on spinal mechanisms that inhibit antagonist muscle activity. These studies suggest that the observed lack of cortical activity witnessed during sustained isometric contraction may be a combination of reduced afferent input, maintenance of the current motor state, and co-contraction mechanisms being located at the spinal level.

Study Limitations

The current experimental design controlled for several confounding factors, such as ordering effects and movement kinematics, that may have influenced the results; however, other factors may have impacted the observed changes in beta-band desynchronization across tasks including stabilization via trunk muscles, EEG contamination by muscle activity, exclusion of true EEG signals, and separation of spinal/supraspinal activity from cortically driven activity. During the study, participants were seated in a chair but were not otherwise restrained. Although participants were monitored throughout the experimental sessions for trunk movements, with none being noted, the setup may have allowed participants to engage stabilizing trunk muscles differently across conditions, eliciting task-specific changes in cortical activity not specifically tied to the arm movement.

Other potential confounding factors arose in the EEG data processing pipeline. During analysis of the EEG data, AMICA was performed to separate the recorded EEG data into signal and artifactual components. It is possible that the AMICA algorithm did not fully separate signal and artifacts, resulting in the removal of some cortical signals and/or the inclusion of some artifactual components in the subsequent source imaging and analysis. This could explain the increase in beta-band power in the lateral occipital region during the CoC task (Fig. 4*B*). During the CoC task, participants displayed increased muscle tension in the arm and neck that may have propagated to posterior EEG recording sites and presented as an increase in beta-band power that was task related and not fully separable using AMICA. In an independent component analysis study examining artifact removal, experts labeled ~17% of independent components as muscle artifact, which makes up ~68% of all artifactual components (Winkler et al. 2011). This equates to ~25% of independent components being artifactual. In our case, we removed an average of 14 independent components from each participant which is ~22% of all components.

Providing visual feedback of the hand during the PER task may have biased the cortical mediated error networks toward visual display errors and resulted in a cortical network utilizing volitional corrections. Behavioral studies where participants have true or shifted visual feedback of their reaching finger toward visual or proprioceptive targets have shown that the false visual feedback has no effect on movements directed toward proprioceptive targets

(Sarlegna and Sainburg 2007; Sober and Sabes 2005). This contrasted with the large reaching errors that result from the visual shift when participants reach for visual targets, suggesting that somatosensory input has a greater influence when participants are planning movements toward proprioceptive targets, whereas visual feedback prevails when they are reaching for visual targets (Sarlegna and Sainburg 2007; Sober and Sabes 2005). If we had done an arm stabilization task without visual feedback, we believe the patterns of cortical network activity would have differed with respect to the primary sensory areas involved in the corrective movement. Specifically, we would have expected the cortically mediated visual error network to shift to a proprioception-based error network located in the somatosensory region (Filimon et al. 2009; Mann et al. 1996), but still including sensory parietal areas (Suminski et al. 2007).

A limitation of this study is the small sample size of only 10 participants. A power analysis conducted before the experiment, using pilot data, found that a sample size of 10 participants provided experimental power for type II error >80% for the variables tested. A post hoc analysis of experimental power for type II error was done and confirmed that the assumed level of variability was consistent with that observed.

Another possible limitation to the study centers around the choice of reference electrode and volume conduction effects associated with the coherence analysis used to characterize functional connectivity. Previous studies (Essl and Rappelsberger 1998; Nunez et al. 1999; Rappelsberger 1989) examining the effect of reference electrode choice have shown that coherence is dependent on the reference electrode or referencing scheme (common average, linked mastoids, etc.). The use of a single electrode as the reference can inflate or deflate coherence values depending on the level of activity at the reference electrode, with higher values at the reference electrode being detrimental to coherence (Zaveri et al. 2000). Rappelsberger (1989) suggested the use of a reference averaging technique, such as linked earlobes, to better approximate a zero-potential reference, which could to help mitigate this issue. Although the common average reference provides an alternative averaging technique, the tendency for EEG signals to be synchronized over large areas of the scalp can result in a common average reference remaining high. Coherence is also impacted by volume conduction effects that result in spatial blurring of cortical point sources measured at the scalp due to the spatial filtering properties of the cerebrospinal fluid, skull, and scalp. Volume conduction results in significant coherence between EEG electrodes that can extend over distances larger than 8 cm (Nunez et al. 1997) even if the cortical regions immediately below the electrodes are not functionally connected. Imaginary coherence (Nolte et al. 2004) and orthogonalization techniques (Brookes et al. 2012; Hipp et al. 2012) can be used to mitigate this issue. In the current study, we chose to examine task-based coherence (Rappelsberger et al. 1994), which effectively subtracts out the baseline level of coherence, along with the volume conduction effect, from the task period coherence (Chen et al. 2003). Although the subtraction approach significantly reduced the impact of the volume conduction artifact on the coherence measure, it rendered near-zero task-based coherence values for adjacent electrodes because of the dominant effect volume conduction has on nearby electrodes (Fig.

5). The impact was minimized, however, by comparing the same connections across tasks rather than different connections within tasks.

During the CoC task, co-contraction during the stabilization period was not sustained at the targeted 10–20% but was instead found to hover around 5%. Throughout the feedback period of the CoC task (0–2 s), it was noted that participants tended to fluctuate their level of co-contraction around the lower threshold of 10%. Once feedback was removed, participants maintained high levels of co-contraction that slowly reduced in magnitude over time. This slow drift continued through the stabilization period (4–6 s). The reduction is consistent with participants' self-reports following testing that sustaining a 10–20% co-contraction was difficult. This indicates a higher than expected effort during the CoC task, which may result from the fact that the levels of co-contraction were normalized by MVC and that people asked to maximally co-contract only produce ~50% of the EMG produced during muscle maximal contraction (Milner et al. 1995; Tyler and Hutton 1986). Another possible explanation may be that the arm was in a different orientation when the co-contraction was being produced during the tasks than when the MVCs were collected. Collecting MVCs in different limb positions has been shown to alter the amount of EMG being produced in the muscle (Boettcher et al. 2008; Buchanan et al. 1989; Singh and Karpovich 1966). Although the level of co-contraction was not sustained at the requested level during the CoC task, the increased levels of co-contraction in the CoC task compared with the PtP task in Fig. 2*B*, together with the participant feedback, indicate that they were actively co-contracting at higher levels than normal throughout the task.

Future Directions

The results reported in this article indicate that stabilization of the arm during visuomotor control of arm posture engages cortical control mechanisms that operate in concert with co-contraction of antagonistic muscles and possibly spinal/supraspinal reflex activity to ensure arm stabilization. We hypothesize that the intermittent voluntary corrections generated by the cortex are the last mechanism recruited to stabilize the arm and are only engaged after the co-contraction of antagonistic muscles and spinal/supraspinal reflex activity mechanisms prove insufficient to adequately stabilize the arm. Future studies could test this hypothesis by utilizing multiple tasks with varying degrees of stabilization difficulty to determine the level of stabilization challenge at which cortical activity and connectivity occurs. We expect a graded increase in co-contraction as well as spinal/supraspinal reflex activity up to a critical point, after which cortical networks would be recruited to help ensure stability.

In future studies, it would also be interesting to examine how stabilization of the arm changes in various disease populations such multiple sclerosis, myelopathy and stroke. Within these populations, the central and/or peripheral nervous system is damaged, resulting in poor motor coordination and stabilization (Conrad et al. 2011a, 2011b). The mechanism to ensure end-point stabilization in these populations may still be intermittent voluntary corrections mediated by a sensorimotor error network, although it may be dysfunctional. Alternatively, control may

be relegated to lower level but functionally intact mechanisms associated with spinal/supraspinal reflexes or co-contraction of antagonistic muscles that may not adequately prevent instability. Previous studies (Conrad et al. 2011a, 2011b) in people with stroke have shown that the application of tendon vibration improves motor control and end-point stabilization while not altering spinal reflex activity (Gadhoke 2011), suggesting that sensory input at the cortical level may be a key factor in arm end-point stabilization.

CONCLUSIONS

In conclusion, maintenance of arm position free of perturbations, co-contraction of the arm, volitional arm movements, and stabilization of the arm are associated with different patterns of brain activation and connectivity. Cortical activity in the sensory, motor, and visual areas during the PER task was similar to that in the VOL task and was larger than the activity in the PtP or CoC task. Similar cortical activity between the VOL and PER tasks suggested the brain might be generating volitional movement commands to stabilize the arm. On the other hand, the PER task had a higher level of network connectivity between the sensorimotor and visual regions compared with the PtP, CoC, and VOL tasks. The difference in cortical connectivity between tasks might be attributed to an underlying visuomotor error network that utilizes visual error information to update the motor commands of the arm. The comparison of cortical activation and connectivity under different conditions indicates the involvement of cortical networks that contribute to visuomotor control of arm posture.

GRANTS

DISCLOSURES

No conflicts of interest, financial or otherwise, are declared by the authors.

AUTHOR CONTRIBUTIONS

D.B.S., S.A.B., and B.D.S. conceived and designed research; D.B.S. performed experiments; D.B.S. analyzed data; D.B.S., S.A.B., and B.D.S. interpreted results of experiments; D.B.S. prepared figures; D.B.S. drafted manuscript; D.B.S., S.A.B., and B.D.S. edited and revised manuscript; D.B.S., S.A.B., and B.D.S. approved final version of manuscript.

AUTHOR NOTES

- Address for reprint requests and other correspondence: B. D. Schmit, PO Box 1881, Milwaukee, WI 53201-1881 (e-mail: brian.schmit@marquette.edu).

REFERENCES

Abbruzzese G, Berardelli A, Rothwell JC, Day BL, Marsden CD. Cerebral potentials and electromyographic responses evoked by stretch of wrist muscles in man. Exp Brain Res 58: 544–551, 1985. doi:10.1007/BF00235870.

Akazawa K, Milner TE, Stein RB. Modulation of reflex EMG and stiffness in response to stretch of human finger muscle. J Neurophysiol 49: 16–27, 1983. doi:10.1152/jn.1983.49.1.16.

Alegre M, Labarga A, Gurtubay IG, Iriarte J, Malanda A, Artieda J. Movement-related changes in cortical oscillatory activity in ballistic, sustained and negative movements. Exp Brain Res 148: 17–25, 2003. doi:10.1007/s00221-002-1255-x.

Baratta RV, Solomonow M, Zhou BH. Frequency domain-based models of skeletal muscle. J Electromyogr Kinesiol 8: 79–91, 1998. doi:10.1016/S1050-6411(97)00024-2.

Boettcher CE, Ginn KA, Cathers I. Standard maximum isometric voluntary contraction tests for normalizing shoulder muscle EMG. J Orthop Res 26: 1591–1597, 2008. doi:10.1002/jor.20675.

Brookes MJ, Woolrich MW, Barnes GR. Measuring functional connectivity in MEG: a multivariate approach insensitive to linear source leakage. Neuroimage 63: 910–920, 2012. doi:10.1016/j.neuroimage.2012.03.048.

Buchanan TS, Rovai GP, Rymer WZ. Strategies for muscle activation during isometric torque generation at the human elbow. J Neurophysiol 62: 1201–1212, 1989. doi:10.1152/jn.1989.62.6.1201.

Chen Y, Ding M, Kelso JA. Task-related power and coherence changes in neuromagnetic activity during visuomotor coordination. Exp Brain Res 148: 105–116, 2003. doi:10.1007/s00221-002-1244-0.

Cheney PD, Fetz EE. Corticomotoneuronal cells contribute to long-latency stretch reflexes in the rhesus monkey. J Physiol 349: 249–272, 1984. doi:10.1113/jphysiol.1984.sp015155.

Christensen MS, Lundbye-Jensen J, Geertsen SS, Petersen TH, Paulson OB, Nielsen JB. Premotor cortex modulates somatosensory cortex during voluntary movements without proprioceptive feedback. Nat Neurosci 10: 417–419, 2007. doi:10.1038/nn1873.

Conrad MO, Scheidt RA, Schmit BD. Effects of wrist tendon vibration on arm tracking in people poststroke. J Neurophysiol 106: 1480–1488, 2011a. doi:10.1152/jn.00404.2010.

Conrad MO, Scheidt RA, Schmit BD. Effects of wrist tendon vibration on targeted upper-arm movements in poststroke hemiparesis. Neurorehabil Neural Repair 25: 61–70, 2011b. doi:10.1177/1545968310378507.

Crago PE, Houk JC, Hasan Z. Regulatory actions of human stretch reflex. J Neurophysiol 39: 925–935, 1976. doi:10.1152/jn.1976.39.5.925.

Cremoux S, Tallet J, Dal Maso F, Berton E, Amarantini D. Impaired corticomuscular coherence during isometric elbow flexion contractions in humans with cervical spinal cord injury. Eur J Neurosci 46: 1991–2000, 2017. doi:10.1111/ejn.13641.

Dawson GD. Cerebral responses to electrical stimulation of peripheral nerve in man. J Neurol Neurosurg Psychiatry 10: 134–140, 1947. doi:10.1136/jnnp.10.3.134.

Delorme A, Makeig S. EEGLAB: an open source toolbox for analysis of single-trial EEG dynamics including independent component analysis. J Neurosci Methods 134: 9–21, 2004. doi:10.1016/j.jneumeth.2003.10.009.

Delorme A, Palmer J, Onton J, Oostenveld R, Makeig S. Independent EEG sources are dipolar. PLoS One 7: e30135, 2012. doi:10.1371/journal.pone.0030135.

Desikan RS, Ségonne F, Fischl B, Quinn BT, Dickerson BC, Blacker D, Buckner RL, Dale AM, Maguire RP, Hyman BT, Albert MS, Killiany RJ. An automated labeling system for subdividing the human cerebral cortex on MRI scans into gyral based regions of interest. Neuroimage 31: 968–980, 2006. doi:10.1016/j.neuroimage.2006.01.021.

Engel AK, Fries P. Beta-band oscillations–signalling the status quo? Curr Opin Neurobiol 20: 156–165, 2010. doi:10.1016/j.conb.2010.02.015.

Essl M, Rappelsberger P. EEG coherence and reference signals: experimental results and mathematical explanations. Med Biol Eng Comput 36: 399–406, 1998. doi:10.1007/BF02523206.

Feldman AG. Once more on the equilibrium-point hypothesis (λ model) for motor control. J Mot Behav 18: 17–54, 1986. doi:10.1080/00222895.1986.10735369.

Filimon F, Nelson JD, Huang RS, Sereno MI. Multiple parietal reach regions in humans: cortical representations for visual and proprioceptive feedback during on-line reaching. J Neurosci 29: 2961–2971, 2009. doi:10.1523/JNEUROSCI.3211-08.2009.

Flash T, Hogan N. The coordination of arm movements: an experimentally confirmed mathematical model. J Neurosci 5: 1688–1703, 1985. doi:10.1523/JNEUROSCI.05-07-01688.1985.

Foley JM, Meyer RA. Energy cost of twitch and tetanic contractions of rat muscle estimated in situ by gated 31P NMR. NMR Biomed 6: 32–38, 1993. doi:10.1002/nbm.1940060106.

Formaggio E, Storti SF, Boscolo Galazzo I, Gandolfi M, Geroin C, Smania N, Spezia L, Waldner A, Fiaschi A, Manganotti P. Modulation of event-related desynchronization in robot-assisted hand performance: brain oscillatory changes in active, passive and imagined movements. J Neuroeng Rehabil 10: 24, 2013. doi:10.1186/1743-0003-10-24.

Franklin DW, Burdet E, Osu R, Kawato M, Milner TE. Functional significance of stiffness in adaptation of multijoint arm movements to stable and unstable dynamics. Exp Brain Res 151: 145–157, 2003a. doi:10.1007/s00221-003-1443-3.

Franklin DW, Osu R, Burdet E, Kawato M, Milner TE. Adaptation to stable and unstable dynamics achieved by combined impedance control and inverse dynamics model. J Neurophysiol 90: 3270–3282, 2003b. doi:10.1152/jn.01112.2002.

Franklin DW, So U, Kawato M, Milner TE. Impedance control balances stability with metabolically costly muscle activation. J Neurophysiol 92: 3097–3105, 2004. doi:10.1152/jn.00364.2004.

Gadhoke B. Role of Tendon Vibration in Multijoint Reflex Coupling in the Hemiparetic Arm Post Stroke (Master's thesis). Milwaukee, WI: Marquette University, 2011.

Ghez C, Shinoda Y. Spinal mechanisms of the functional stretch reflex. Exp Brain Res 32: 55–68, 1978. doi:10.1007/BF00237390.

Giblin DR. Somatosensory evoked potentials in healthy subjects and in patients with lesions of the nervous system. Ann N Y Acad Sci 112: 93–142, 1964. doi:10.1111/j.1749-6632.1964.tb26744.x.

Gilbertson T, Lalo E, Doyle L, Di Lazzaro V, Cioni B, Brown P. Existing motor state is favored at the expense of new movement during 13-35 Hz oscillatory synchrony in the human corticospinal system. J Neurosci 25: 7771–7779, 2005. doi:10.1523/JNEUROSCI.1762-05.2005.

Gourab K, Schmit BD. Changes in movement-related β-band EEG signals in human spinal cord injury. Clin Neurophysiol 121: 2017–2023, 2010. doi:10.1016/j.clinph.2010.05.012.

Gramfort A, Papadopoulo T, Olivi E, Clerc M. OpenMEEG: opensource software for quasistatic bioelectromagnetics. Biomed Eng Online 9: 45, 2010. doi:10.1186/1475-925X-9-45.

Gribble PL, Mullin LI, Cothros N, Mattar A. Role of cocontraction in arm movement accuracy. J Neurophysiol 89: 2396–2405, 2003. doi:10.1152/jn.01020.2002.

Guzzetta A, Staudt M, Petacchi E, Ehlers J, Erb M, Wilke M, Krägeloh-Mann I, Cioni G. Brain representation of active and passive hand movements in children. Pediatr Res 61: 485–490, 2007. doi:10.1203/pdr.0b013e3180332c2e.

Gwin JT, Ferris DP. An EEG-based study of discrete isometric and isotonic human lower limb muscle contractions. J Neuroeng Rehabil 9: 35, 2012. doi:10.1186/1743-0003-9-35.

Hämäläinen MS, Ilmoniemi RJ. Interpreting magnetic fields of the brain: minimum norm estimates. Med Biol Eng Comput 32: 35–42, 1994. doi:10.1007/BF02512476.

Hasan Z. The human motor control system's response to mechanical perturbation: should it, can it, and does it ensure stability? J Mot Behav 37: 484–493, 2005. doi:10.3200/JMBR.37.6.484-493.

Hidler JM, Rymer WZ. A simulation study of reflex instability in spasticity: origins of clonus. IEEE Trans Rehabil Eng 7: 327–340, 1999. doi:10.1109/86.788469.

Hipp JF, Hawellek DJ, Corbetta M, Siegel M, Engel AK. Large-scale cortical correlation structure of spontaneous oscillatory activity. Nat Neurosci 15: 884–890, 2012. doi:10.1038/nn.3101.

Hof AL. In vivo measurement of the series elasticity release curve of human triceps surae muscle. J Biomech 31: 793–800, 1998. doi:10.1016/S0021-9290(98)00062-1.

Hogan MC, Kurdak SS, Arthur PG. Effect of gradual reduction in O_2 delivery on intracellular homeostasis in contracting skeletal muscle. J Appl Physiol (1985) 80: 1313–1321, 1996. doi:10.1152/jappl.1996.80.4.1313.

Hogan N. Adaptive control of mechanical impedance by coactivation of antagonist muscles. IEEE Trans Automat Contr 29: 681–690, 1984. doi:10.1109/TAC.1984.1103644.

Houk JC, Fagg AH, Barto AG. Fractional power damping model of joint motion. In: Progress in Motor Control: Structure-Function Relations in Voluntary Movements, edited by Latash ML. Champaign, IL: Human Kinetics, 2000, p. 147–178.

Kalaska JF, Scott SH, Cisek P, Sergio LE. Cortical control of reaching movements. Curr Opin Neurobiol 7: 849–859, 1997. doi:10.1016/S0959-4388(97)80146-8.

Kornhuber HH, Deecke L. Brain potential changes in voluntary and passive movements in humans: readiness potential and reafferent potentials. Pflugers Arch 468: 1115–1124, 2016. doi:10.1007/s00424-016-1852-3.

Koshland GF, Hasan Z, Gerilovsky L. Activity of wrist muscles elicited during imposed or voluntary movements about the elbow joint. J Mot Behav 23: 91–100, 1991. doi:10.1080/00222895.1991.9942026.

Kurtzer IL, Pruszynski JA, Scott SH. Long-latency reflexes of the human arm reflect an internal model of limb dynamics. Curr Biol 18: 449–453, 2008. doi:10.1016/j.cub.2008.02.053.

Kybic J, Clerc M, Abboud T, Faugeras O, Keriven R, Papadopoulo T. A common formalism for the integral formulations of the forward EEG problem. IEEE Trans Med Imaging 24: 12–28, 2005. doi:10.1109/TMI.2004.837363.

Lacquaniti F, Soechting JF. Behavior of the stretch reflex in a multi-jointed limb. Brain Res 311: 161–166, 1984. doi:10.1016/0006-8993(84)91411-2.

Lacquaniti F, Soechting JF. EMG responses to load perturbations of the upper limb: effect of dynamic coupling between shoulder and elbow motion. Exp Brain Res 61: 482–496, 1986. doi:10.1007/BF00237573.

Latash ML. The organization of quick corrections within a two-joint synergy in conditions of unexpected blocking and release of a fast movement. Clin Neurophysiol 111: 975–987, 2000. doi:10.1016/S1388-2457(00)00263-7.

Latash ML, Levin MF, Scholz JP, Schöner G. Motor control theories and their applications. Medicina (Kaunas) 46: 382–392, 2010. doi:10.3390/medicina46060054.

Lee JJ, Schmit BD. Effect of sensory attenuation on cortical movement-related oscillations. J Neurophysiol 119: 971–978, 2018. doi:10.1152/jn.00171.2017.

Loram ID, Lakie M. Human balancing of an inverted pendulum: position control by small, ballistic-like, throw and catch movements. J Physiol 540: 1111–1124, 2002. doi:10.1113/jphysiol.2001.013077.

Makeig S, Debener S, Onton J, Delorme A. Mining event-related brain dynamics. Trends Cogn Sci 8: 204–210, 2004. doi:10.1016/j.tics.2004.03.008.

Mann CA, Sterman MB, Kaiser DA. Suppression of EEG rhythmic frequencies during somato-motor and visuo-motor behavior. Int J Psychophysiol 23: 1–7, 1996. doi:10.1016/0167-8760(96)00036-0.

Marsden CD, Rothwell JC, Day BL. Long-latency automatic responses to muscle stretch in man: origin and function. Adv Neurol 39: 509–539, 1983.

McFarland DJ, Miner LA, Vaughan TM, Wolpaw JR. Mu and beta rhythm topographies during motor imagery and actual movements. Brain Topogr 12: 177–186, 2000. doi:10.1023/A:1023437823106.

Milner TE, Cloutier C, Leger AB, Franklin DW. Inability to activate muscles maximally during cocontraction and the effect on joint stiffness. Exp Brain Res 107: 293–305, 1995. doi:10.1007/BF00230049.

Mognon A, Jovicich J, Bruzzone L, Buiatti M. ADJUST: an automatic EEG artifact detector based on the joint use of spatial and temporal features. Psychophysiology 48: 229–240, 2011. doi:10.1111/j.1469-8986.2010.01061.x.

Morasso PG, Schieppati M. Can muscle stiffness alone stabilize upright standing? J Neurophysiol 82: 1622–1626, 1999. doi:10.1152/jn.1999.82.3.1622.

Morasso PG, Sanguineti V. Ankle muscle stiffness alone cannot stabilize balance during quiet standing. J Neurophysiol 88: 2157–2162, 2002. doi:10.1152/jn.2002.88.4.2157.

Mortimer JA, Webster DD, Dukich TG. Changes in short and long latency stretch responses during the transition from posture to movement. Brain Res 229: 337–351, 1981. doi:10.1016/0006-8993(81)90998-7.

Mutha PK, Boulinguez P, Sainburg RL. Visual modulation of proprioceptive reflexes during movement. Brain Res 1246: 54–69, 2008. doi:10.1016/j.brainres.2008.09.061.

Nolte G, Bai O, Wheaton L, Mari Z, Vorbach S, Hallett M. Identifying true brain interaction from EEG data using the imaginary part of coherency. Clin Neurophysiol 115: 2292–2307, 2004. doi:10.1016/j.clinph.2004.04.029.

Nunez PL, Silberstein RB, Shi Z, Carpenter MR, Srinivasan R, Tucker DM, Doran SM, Cadusch PJ, Wijesinghe RS. EEG coherency II: experimental comparisons of multiple measures. Clin Neurophysiol 110: 469–486, 1999. doi:10.1016/S1388-2457(98)00043-1.

Nunez PL, Srinivasan R, Westdorp AF, Wijesinghe RS, Tucker DM, Silberstein RB, Cadusch PJ. EEG coherency. I: Statistics, reference electrode, volume conduction, Laplacians, cortical imaging, and interpretation at multiple scales. Electroencephalogr Clin Neurophysiol 103: 499–515, 1997. doi:10.1016/S0013-4694(97)00066-7.

O'Neill GC, Tewarie PK, Colclough GL, Gascoyne LE, Hunt BAE, Morris PG, Woolrich MW, Brookes MJ. Measurement of dynamic task related functional networks using MEG. Neuroimage 146: 667–678, 2017. doi:10.1016/j.neuroimage.2016.08.061.

Oostenveld R, Fries P, Maris E, Schoffelen JM. FieldTrip: open source software for advanced analysis of MEG, EEG, and invasive electrophysiological data. Comput Intell Neurosci 2011: 156869, 2011. doi:10.1155/2011/156869.

Palmer JA, Makeig S, Kreutz-Delgado K, Rao BD. Newton method for the ICA mixture model. In: 2008 IEEE International Conference on Acoustics, Speech and Signal Processing. 2008: 1805–1808, 2008. doi:10.1109/ICASSP.2008.4517982.

Pfluger E. Die sensoriscen Functionen des Rückenmarks bei Wirbelttieren nebst einer neuen Lehre über die Leitungsgesetze der Reflecxionen. Berlin: Hirschwald, 1853.

Pfurtscheller G, Lopes da Silva F. Functional meaning of event-related desynchronization (ERD) end synchronization (ERS). In: Event-Related Desynchronization. Handbook of Electroencephalography and Clinical Neurophysiology, edited by Pfurtscheller G, Lopes da Silva F. Amsterdam: Elsevier, 1999a, vol. 6, p. 51–66.

Pfurtscheller G, Lopes da Silva FH. Event-related EEG/MEG synchronization and desynchronization: basic principles. Clin Neurophysiol 110: 1842–1857, 1999b. doi:10.1016/S1388-2457(99)00141-8.

Pfurtscheller G, Neuper C, Andrew C, Edlinger G. Foot and hand area mu rhythms. Int J Psychophysiol 26: 121–135, 1997. doi:10.1016/S0167-8760(97)00760-5.

Pfurtscheller G, Neuper C, Mohl W. Event-related desynchronization (ERD) during visual processing. Int J Psychophysiol 16: 147–153, 1994. doi:10.1016/0167-8760(89)90041-X.

Pfurtscheller G, Pichler-Zalaudek K, Neuper C. ERD and ERS in voluntary movement of different limbs. In: Event-Related Desynchronization. Handbook of Electroencephalography and Clinical Neurophysiology, edited by Pfurtscheller G, Lopes da Silva F. Amsterdam: Elsevier, 1999, vol. 6, p. 245–268.

Platz T, Kim IH, Pintschovius H, Winter T, Kieselbach A, Villringer K, Kurth R, Mauritz KH. Multimodal EEG analysis in man suggests impairment-specific changes in movement-related electric brain activity after stroke. Brain 123: 2475–2490, 2000. doi:10.1093/brain/123.12.2475.

Pogosyan A, Gaynor LD, Eusebio A, Brown P. Boosting cortical activity at beta-band frequencies slows movement in humans. Curr Biol 19: 1637–1641, 2009. doi:10.1016/j.cub.2009.07.074.

Pruszynski JA, Kurtzer I, Nashed JY, Omrani M, Brouwer B, Scott SH. Primary motor cortex underlies sensory integration for fast feedback control. Nature 478: 387–391, 2011a. doi:10.1038/nature10436.

Pruszynski JA, Kurtzer I, Scott SH. Rapid motor responses are appropriately tuned to the metrics of a visuospatial task. J Neurophysiol 100: 224–238, 2008. doi:10.1152/jn.90262.2008.

Pruszynski JA, Kurtzer I, Scott SH. The long-latency reflex is composed of at least two functionally independent processes. J Neurophysiol 106: 449–459, 2011b. doi:10.1152/jn.01052.2010.

Puce A, Hämäläinen MS. A review of issues related to data acquisition and analysis in EEG/MEG studies. Brain Sci 7: 58, 2017. doi:10.3390/brainsci7060058.

Rappelsberger P. The reference problem and mapping of coherence: a simulation study. Brain Topogr 2: 63–72, 1989. doi:10.1007/BF01128844.

Rappelsberger P, Lacroix D, Petsche H. Amplitude and coherence mapping: its application in psycho- and patho-physiological studies. In: Quantitative EEG Analysis: Clinical Utility and New Methods, edited by Rother M, Zwiener U. Jena, Germany: Jena Universitätsverlag, 1993, p. 179–186.

Rappelsberger P, Pfurtscheller G, Filz O. Calculation of event-related coherence–a new method to study short-lasting coupling between brain areas. Brain Topogr 7: 121–127, 1994. doi:10.1007/BF01186770.

Sainburg RL. Evidence for a dynamic-dominance hypothesis of handedness. Exp Brain Res 142: 241–258, 2002. doi:10.1007/s00221-001-0913-8.

Sainburg RL. Handedness: differential specializations for control of trajectory and position. Exerc Sport Sci Rev 33: 206–213, 2005. doi:10.1097/00003677-200510000-00010.

Sarlegna FR, Sainburg RL. The effect of target modality on visual and proprioceptive contributions to the control of movement distance. Exp Brain Res 176: 267–280, 2007. doi:10.1007/s00221-006-0613-5.

Scheidt RA, Ghez C. Separate adaptive mechanisms for controlling trajectory and final position in reaching. J Neurophysiol 98: 3600–3613, 2007. doi:10.1152/jn.00121.2007.

Shadmehr R, Smith MA, Krakauer JW. Error correction, sensory prediction, and adaptation in motor control. Annu Rev Neurosci 33: 89–108, 2010. doi:10.1146/annurev-neuro-060909-153135.

Shemmell J, An JH, Perreault EJ. The differential role of motor cortex in stretch reflex modulation induced by changes in environmental mechanics and verbal instruction. J Neurosci 29: 13255–13263, 2009. doi:10.1523/JNEUROSCI.0892-09.2009.

Sih BL, Stuhmiller JH. The metabolic cost of force generation. Med Sci Sports Exerc 35: 623–629, 2003. doi:10.1249/01.MSS.0000058435.67376.49.

Singh M, Karpovich PV. Isotonic and isometric forces of forearm flexors and extensors. J Appl Physiol 21: 1435–1437, 1966. doi:10.1152/jappl.1966.21.4.1435.

Sober SJ, Sabes PN. Flexible strategies for sensory integration during motor planning. Nat Neurosci 8: 490–497, 2005. doi:10.1038/nn1427.

Soechting JF, Dufresne JR, Lacquaniti F. Time-varying properties of myotatic response in man during some simple motor tasks. J Neurophysiol 46: 1226–1243, 1981. doi:10.1152/jn.1981.46.6.1226.

Spieser L, Meziane HB, Bonnard M. Cortical mechanisms underlying stretch reflex adaptation to intention: a combined EEG-TMS study. Neuroimage 52: 316–325, 2010. doi:10.1016/j.neuroimage.2010.04.020.

Stein PS, Grossman ML. Central program for scratch reflex in turtle. J Comp Physiol 140: 287–294, 1980. doi:10.1007/BF00606269.

Steriade M, Gloor P, Llinás RR, Lopes da Silva FH, Mesulam MM. Report of IFCN Committee on Basic Mechanisms. Basic mechanisms of cerebral rhythmic activities. Electroencephalogr Clin Neurophysiol 76: 481–508, 1990. doi:10.1016/0013-4694(90)90001-Z.

Sukerkar P. EEG Source Localization of Visual and Proprioceptive Error Processing During Visually-Guided Target Tracking with the Wrist (Master's thesis). Milwaukee, WI: Marquette University, 2010.

Suminski AJ, Rao SM, Mosier KM, Scheidt RA. Neural and electromyographic correlates of wrist posture control. J Neurophysiol 97: 1527–1545, 2007. doi:10.1152/jn.01160.2006.

Swann N, Tandon N, Canolty R, Ellmore TM, McEvoy LK, Dreyer S, DiSano M, Aron AR. Intracranial EEG reveals a time- and frequency-specific role for the right inferior frontal gyrus and primary motor cortex in stopping initiated responses. J Neurosci 29: 12675–12685, 2009. doi:10.1523/JNEUROSCI.3359-09.2009.

Tadel F, Baillet S, Mosher JC, Pantazis D, Leahy RM. Brainstorm: a user-friendly application for MEG/EEG analysis. Comput Intell Neurosci 2011: 879716, 2011. doi:10.1155/2011/879716.

Todorov E, Jordan MI. Optimal feedback control as a theory of motor coordination. Nat Neurosci 5: 1226–1235, 2002. doi:10.1038/nn963.

Tracey DJ, Walmsley B, Brinkman J. 'Long-loop' reflexes can be obtained in spinal monkeys. Neurosci Lett 18: 59–65, 1980. doi:10.1016/0304-3940(80)90213-X.

Tyler AE, Hutton RS. Was Sherrington right about co-contractions? Brain Res 370: 171–175, 1986. doi:10.1016/0006-8993(86)91119-4.

Weiller C, Jüptner M, Fellows S, Rijntjes M, Leonhardt G, Kiebel S, Müller S, Diener HC, Thilmann AF. Brain representation of active and passive movements. Neuroimage 4: 105–110, 1996. doi:10.1006/nimg.1996.0034.

Wierzbicka MM, Wiegner AW. Effects of weak antagonist on fast elbow flexion movements in man. Exp Brain Res 91: 509–519, 1992. doi:10.1007/BF00227847.

Wierzbicka MM, Wiegner AW. Accuracy of motor responses in subjects with and without control of antagonist muscle. J Neurophysiol 75: 2533–2541, 1996. doi:10.1152/jn.1996.75.6.2533.

Winkler I, Haufe S, Tangermann M. Automatic classification of artifactual ICA-components for artifact removal in EEG signals. Behav Brain Funct 7: 30, 2011. doi:10.1186/1744-9081-7-30.

Yuan H, Liu T, Szarkowski R, Rios C, Ashe J, He B. Negative covariation between task-related responses in alpha/beta-band activity and BOLD in human sensorimotor cortex: an EEG and fMRI study of motor imagery and movements. Neuroimage 49: 2596–2606, 2010. doi:10.1016/j.neuroimage.2009.10.028.

Zaveri HP, Duckrow RB, Spencer SS. The effect of a scalp reference signal on coherence measurements of intracranial electroencephalograms. Clin Neurophysiol 111: 1293–1299, 2000. doi:10.1016/S1388-2457(00)00321-7.

Zhou B, Wong WH. A bootstrap-based non-parametric ANOVA method with applications to factorial microarray data. Stat Sin 21: 495–514, 2011. doi:10.5705/ss.2011.023a.